Osteology of Aristonectes quiriquinensis (Elasmosauridae, Aristonectinae) from the upper Maastrichtian of central Chile

Rodrigo A. Otero, Sergio Soto-Acuña & Frank R. O'keefe

ARTICLE

OSTEOLOGY OF *ARISTONECTES QUIRIQUINENSIS* (ELASMOSAURIDAE, ARISTONECTINAE) FROM THE UPPER MAASTRICHTIAN OF CENTRAL CHILE

RODRIGO A. OTERO,*[1] SERGIO SOTO-ACUÑA,[1,2] and FRANK R. O'KEEFE[3]
[1]Laboratorio de Ontogenia y Filogenia, Departamento de Biología, Facultad de Ciencias, Universidad de Chile, Las Palmeras 3425, Santiago 7800003, Chile, otero2112@gmail.com; arcosaurio@gmail.com
[2]Comisión de Patrimonio Natural, Consejo de Monumentos Nacionales, Av. Vicuña Mackena 084, Santiago 7500910, Chile, ssoto@monumentos.cl;
[3]Department of Biological Sciences, Marshall University, One John Marshall Drive, Huntington, West Virginia 25755, U.S.A., okeefef@marshall.edu

ABSTRACT—The upper Maastrichtian elasmosaurid plesiosaur *Aristonectes quiriquinensis* from central Chile is here redescribed following further preparation of the holotype. New cranial characters include a flattened skull with a caudal extension of the mandibular articulation far posterior to the occipital condyle; a very long, horizontal, and posteriorly oriented paroccipital process; mandible with restricted gape angle; and teeth oriented rostrally and not interlocking during occlusion. Postcranial features include the presence of very long extremities (ca. 3 m), whereas features of the caudal-most vertebrae suggest the presence of a horizontal caudal fin. Additionally, neuroanatomical features of *Aristonectes* are for the first time described based on a braincase cast. Integration of osteological features, anatomical comparisons, as well as taphonomic and environmental data strongly suggests that the foraging behavior of *Aristonectes quiriquinensis* incorporated a mix of engulfment and feeding from benthic sediments. This is a novelty among elasmosaurids, so far considered as mainly epipelagic feeders.

SUPPLEMENTAL DATA—Supplemental materials are available for this article for free at www.tandfonline.com/UJVP

INTRODUCTION

Aristonectinae is a clade of highly derived elasmosaurid plesiosaurs found in upper Campanian–Maastrichtian (70–65 Ma) sediments, exclusively along the Southern Hemisphere, in a geoecologic realm known as the Weddellian Province (Zinsmeister, 1979). So far, the group includes *Kaiwhekea katiki* Cruickshank and Fordyce, 2002 and a juvenile postcranial specimen (O'Gorman et al., 2014b), both from the lower Maastrichtian of New Zealand. Adding to this, the fragmentary skull CM Zfr 73 and 91, holotype of *Alexandronectes zealandiensis* Otero et al., 2016, also from the lower Maastrichtian of New Zealand, represents a basal aristonectine. Three aristonectine taxa with flattened skulls are known. Two of them have been found to be congeneric and respectively belong to the species *Aristonectes parvidens* Cabrera, 1941 from the upper Maastrichtian of Chubut, Argentina (Gasparini et al., 2003), and *Aristonectes quiriquinensis* Otero et al., 2014c from the upper Maastrichtian of central Chile. A last taxon with flattened skull is represented by TTU P9219, recovered from upper Maastrichtian beds of Seymour Island, Antarctica. That specimen was first identified as a new genus and species, *Morturneria seymourensis*, by Chatterjee and Small (1989) but later reinterpreted as a juvenile individual of *Aristonectes parvidens* by Gasparini et al. (2003). The original identification was

recently reassessed and considered as valid by O'Keefe et al. (2017). In addition, indeterminate aristonectines have been reported from upper Campanian levels of the Santa Marta Formation, James Ross Island, Antarctica (Otero et al., 2014c).

Postcranial remains of aristonectines have also been collected from upper Campanian and upper Maastrichtian beds from all the mentioned localities (O'Gorman et al., 2013; O'Gorman et al., 2014a; O'Gorman et al., 2014b; Otero et al., 2012; Otero et al., 2014a), supporting a high abundance of the group in the Southern Hemisphere during the Late Cretaceous. Additionally, several specimens from the lower Maastrichtian of Angola have been referred to indeterminate aristonectines by Araújo et al. (2015).

This article presents new osteological features of *Aristonectes quiriquinensis*. The skull anatomy radically differs from its first description (Otero et al., 2014c) in possessing highly derived features that are not seen in other aristonectines. Additional new features of the postcranial skeleton are also presented. Previously recognized skull features of the genus *Aristonectes* already indicated a specialized feeding behavior. However, the new evidence presented here suggests that *Aristonectes quiriquinensis* was a bottom feeder, likely probing benthic sediments in search of small, soft-bodied prey.

LOCALITY AND GEOLOGIC SETTING

The holotype of *Aristonectes quiriquinensis* (SGO.PV.957) was recovered from limestones exposed on the coast of the locality of Cocholgüe, in the Biobío Region of central Chile, 400 km south of Santiago (Fig. 1). That interval belongs to the upper

---

*Corresponding author.

Color versions of one or more of the figures in this article can be found online at www.tandfonline.com/ujvp.
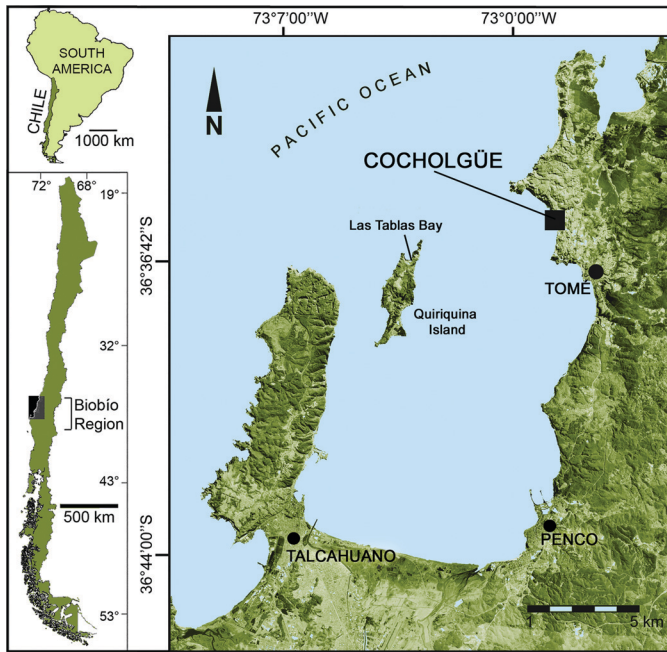
FIGURE 1. Map of the bay of Concepción, Biobío Region, central Chile. Holotype locality at Cocholgüe marked by a square (36°35′40″ S; 72°58′40″ W).

section of the Quiriquina Formation (Biró-Bagózcky, 1982), with Cocholgüe considered the paratype locality of the unit. The referred juvenile specimen (SGO.PV.260) was recovered from the Quiriquina Island near Cocholgüe, from strata belonging to the same unit. The Quiriquina Formation was first assigned to the Campanian–Maastrichtian based on abundant and diverse ammonoids and bivalves (e.g., Biró-Bagóczky, 1982). Subsequent revisions of the ammonoid assemblage refined the age to the Maastrichtian (Stinnesbeck, 1986) and then to the upper Maastrichtian (Stinnesbeck, 1996; Salazar et al., 2010; Stinnesbeck et al., 2012).

MATERIAL AND METHODS

The holotype of *Aristonectes quiriquinensis* (SGO.PV.957) is a largely complete skeleton including a partial skull, most of the neck, forelimbs, scattered elements of the trunk, and one incomplete hind limb. The skull was mechanically prepared (K. E. Buldrini and J. Alarcón, Museo Nacional de Historia Natural de Santiago, between 2013 and 2015) with hand tools. A few previously undescribed skull fragments were also recovered from matrix and have been added to the specimen. Additional preparation of the tail of SGO.PV.260 (referred) was carried out during 2014, adding a few postcranial features to the osteological description. After preparation of the skull, an internal cast of the braincase was obtained using dental silicon (Xantoprene). Because the left side of the skull is crushed, the cast was digitally mirrored following its midline, obtaining a symmetric representation. Anatomical identification of the internal braincase elements follows Hopson (1979) and Ten Donkelaar (1998). Osteological comparison between adult and juvenile ontogenetic stages was based on the fairly complete postcranial skeleton SGO.PV.260, referred to *Aristonectes quiriquinensis* (Otero et al., 2012; Otero et al., 2014c).

Phylogenetic analysis is based on the data matrix of Benson and Druckenmiller (2014), introducing the modifications by Otero (2016) and correcting few errors included in the latter (Supplementary Data 1). Some characters regarding the orbit,

the temporal fenestra, and the jugal bar of *Aristonectes parvidens* are based on a speculative reconstruction originally proposed by Ángel Cabrera (Universidad de La Plata, Argentina) for exhibition of the specimen. The reconstruction may be erroneous given what we now know about skulls of other aristonectines (i.e., *Kaiwhekea katiki*, *Aristonectes quiriquinensis*, and TTU P9219). We revised the scoring of *Aristonectes parvidens* based on direct review of the specimen. In our revised scoring, the characters regarding the mentioned elements have been marked as unknown. Additionally, new states for several characters are proposed (Table 1) based on the new features observed on *Aristonectes quiriquinensis*. The analysis was performed using TNT software version 1.1 (Goloboff et al., 2003). Preliminary analyses considered traditional search (Wagner trees, 1,000 replicates; 1,000 trees to save per replication) and bootstrap resampling (2,000 replicates, standard option).

Institutional Abbreviations—GWWU, Geomuseum der Westfälische Wilhems-Universität, Münster, Germany; **NHMUK**, Natural History Museum, London, U.K.; **SGO.PV**, Museo Nacional de Historia Natural, Santiago, Chile; **TTU P**, Museum of Texas, Tech University, Lubbock, Texas, U.S.A.

SYSTEMATIC PALEONTOLOGY

DIAPSIDA Osborn, 1903
SAUROPTERYGIA Owen, 1860
PLESIOSAURIA Blainville, 1835
PLESIOSAUROIDEA Welles, 1943
XENOPSARIA Benson and Druckenmiller, 2014
ELASMOSAURIDAE Cope, 1869
ARISTONECTINAE O'Keefe and Street, 2009 (sensu Otero, Soto-Acuña, and Rubilar-Rogers, 2012)
Genus *ARISTONECTES* Cabrera, 1941

Type Species—*Aristonectes parvidens* Cabrera, 1941. MLP 40-XI-14-6 (holotype), part of a skull attached to the mandible, atlas-axis, and 21 other cervical vertebrae of which the anterior 16 are articulated, eight caudal vertebrae, and an incomplete limb. Cañadón del Loro, northwestern Chubut province, Argentina. Paso del Sapo Formation, Lefipan Member, Maastrichtian (Gasparini et al., 2003).

ARISTONECTES QUIRIQUINENSIS Otero et al., 2014c
(Figs. 2–11)

Holotype—SGO.PV.957. Skeleton including the skull, atlas-axis, 12 anterior cervical vertebrae, 23 mid-to-posterior cervical vertebrae, most of the trunk, both almost complete forelimbs, and most of the proximal portion of the right hind limb.

Locality—Cocholgüe, Biobío Region, central Chile.

Horizon and Age—Upper levels of the Quiriquina Formation (Biró-Bagóczky, 1982), upper Maastrichtian.

Referred Specimens—SGO.PV.260, a fairly complete postcranial skeleton lacking the skull and half of the neck; SGO.PV.135, a complete femur; SGO.PV.169, a proximal portion of a humerus (Otero, O'Gorman, and Hiller, 2015); SGO.PV.94, an anterior caudal series. Las Tablas Bay, upper levels of the Quiriquina Formation, upper Maastrichtian.

Emended Diagnosis—The following new features resulted from additional preparation and re-study of the skull. This new combination of characters is so far unique to *Aristonectes quiriquinensis*: posterolateral ends of the skull and mandibular rami extended far posterior to the occipital condyle, forming a table-like structure with contribution of the pterygoids and squamosals and posteriorly enclosing each temporal fenestra; squamosal anteriorly extending into the lateral walls of the braincase and not forming a squamosal arch as in other plesiosaurs; posterior end of interpterygoid vacuities not enclosed by pterygoids

TABLE 1. Character modifications applied to the data matrix of Benson and Druckenmiller (2014).

Character number	Original description (Benson and Druckenmiller, 2014)	Modification	References
8	Inclination of the suspensorium: subvertical or weakly inclined (~80–90°) (0); significantly inclined (<70°) (1)	New state: (2) suspensorium absent, squamosals join the pterygoids and parietals	Carpenter (1999, character 9), Sato (2002, character 75), Druckenmiller and Russell (2008, character 36), Ketchum and Benson (2010, character 45)
49	Intersquamosal suture along the dorsal midline in lateral view: low and rounded (0); raised approximately one-third orbit height dorsally relative to skull table (1); raised abruptly and substantially dorsally relative to skull table (2)	New state: (3) squamosals join the parietals	State 2 taken from Benson, Ketchum, et al. (2012, character 43)
53	Squamosal arch, posterior margin in dorsal view: dorsal processes extend anterolaterally (0); approximately straight, squamosal dorsal processes extend laterally from midline contact (1); 'V'-shaped, squamosal dorsal processes extend posterolaterally (2)	New state: (3) squamosals do not meet dorsomedially	Benson and Druckenmiller (2014).
70	Opisthotic, paroccipital process length relative to height of exoccipital body: subequal (0); long, at least 1.3 times as long as body height (1)	New state: (2) over three times the height of the exoccipital-opisthotic	Benson et al. (2012a, character 53); modified from O'Keefe (2001, character 46), Sato (2002, character 64), O'Keefe and Wahl (2003, character 24), Großmann (2007, character 21), Druckenmiller and Russell (2008, character 61), Smith and Dyke (2008, character 49)
71	Opisthotic, orientation of paroccipital process relative to ventral surface of exoccipital in posterior view: inclined dorsally (0); paroccipital process oriented parallel to ventral surface of exoccipital (1); inclined ventrally (2)	New state: (3) posteriorly straight	Benson et al. (2012a, character 54); modified from O'Keefe (2001, character 48), Sato (2002, character 67), O'Keefe and Wahl (2003, character 26), Großmann (2007, character 22), Druckenmiller and Russell (2008, character 65), O'Keefe and Street (2009, character 22), Ketchum and Benson (2010, character 77)
72	Opisthotic, morphology of articulation with suspensorium: anterior surface of expanded lateral end makes broad contact with suspensorium (0); lateral end unexpanded, lateral/terminal surface makes narrow contact with suspensorium (1)	New state: (2) long contact along half of the lateromedial margin of the paroccipital process	Benson et al. (2012a, character 55); modified from O'Keefe (2001, character 49), O'Keefe and Wahl (2003, character 27)
73	Opisthotic, shaft of paroccipital process cross section: subcircular, dorsoventral height subequal to anteroposterior width (0); dorsoventrally flattened; anteroposterior width much greater than dorsoventral height (1)	New state: (2) proximally subcircular and distally flattened	Benson et al. (2012a, character 56)
87	Suborbital fenestra bordered by ectopterygoid and maxilla: absent (0); present (1)	New state: (2) parasphenoid extended broad and anterior to the posterior margin of the interpterygoid vacuities through a medial projection	O'Keefe (2001, character 82), Sato (2002, character 45), O'Keefe and Wahl (2003, character 46), Druckenmiller and Russell (2008, character 44), Smith and Dyke (2008, character 40), O'Keefe and Street (2009, character 37), Ketchum and Benson (2010, character 55), Benson et al. (2012a, character 66)
109	Ectopterygoid/pterygoid boss/flange: absent (0); ventrally deflected posterior margin forms flange (1); rugose ventral boss present (2)	New state: (3) ectopterygoid forms a flange mostly with palatine and has a scarce contact with pterygoid	Benson et al. (2012a, character 84); modified from O'Keefe (2001, character 84), Sato (2002, character 57), Druckenmiller and Russell (2008, character 47), Ketchum and Benson (2010, character 58) by interposition of state 1 from Sato (2002, character 56).
163	Cervical ribs, size and orientation of distal processes: marked anterior and posterior processes throughout cervical rib series, combined long axis of processes oriented approximately anteroposteriorly (0); processes reduced, especially anterior process, combined long axis oriented posteroventrally (1); large, anteroposteriorly expansive, sheet-like ribs with prominent processes (2)	New state: (3) cervical ribs without anterior process but inflected rostrally	Otero et al. (2014c, character 59); modified from O'Keefe and Street (2009). Modified from characters describing the presence and morphology of the anterior process: O'Keefe (2001, character 123), Sato (2002, character 146), O'Keefe and Wahl (2003, character 68), Druckenmiller and Russell (2008, character 115), Smith and Dyke (2008, character 71), O'Keefe and Street (2009, character 59), Ketchum and Benson (2010, character 134), Vincent et al. (2011, character 52), Benson et al. (2012a, character 124)

TABLE 1. Character modifications applied to the data matrix of Benson and Druckenmiller (2014). *(Continued)*

Character number	Original description (Benson and Druckenmiller, 2014)	Modification	References
189	Caudal centra, outline of middle caudal centra in anterior view: suboval (0); subrectangular, chevron facets widely spaced and located ventrolaterally, ventral surface approximately flat giving a subrectangular appearance to centrum in anterior view (1)	New state: (2) octagonal outline due to large facets of the neural arch and ribs, plus presence of a flattened ventral surface	Benson et al. (2012a, character 150)

meeting in the midline. Its posterior end is not closed, whereas the internal surface (formed by basioccipital and parasphenoid) is recurved dorsally and ends in the articular margin between the basioccipital and the atlas-axis; paroccipital processes with its distal half fused to the squamosals and contacting the dorsal-most point of the squamosals; exoccipital-opistothics recurved rostrally. These features add to the previous skull autapomorphies (Otero et al., 2014c), represented by a head proportionally smaller than that of *A. parvidens*, having larger cervical vertebrae and the skull more reduced; presence of a symphyseal pit (former mental boss, see further text) on the anteroventral surface of the symphysis, which is not present in *A. parvidens*; absence of lingual platform in ventral view, which is present in A. parvidens (Gasparini et al., 2003:fig. 2b); and the anterior portion of the mandible more dorsoventrally compressed than in *A. parvidens* (Gasparini et al., 2003:fig. 2a).

Unique postcranial features here provided includes an approximate axial formula of 109 centra with 43 cervical, three pectoral, 24 dorsal, three (estimated) sacral, and 35 caudal vertebrae, differing from most elasmosaurids, which possess 18 or 19 dorsal vertebrae and a variable number of cervical vertebrae greater than 50; neural spines as well as cervical ribs both strongly recurved cranially; humeri and femora with hemispherical articular heads. Anterior caudal centra broader than high or long, with octagonal outline has been previously considered as diagnostic of the genus *Aristonectes* (Otero and O'Gorman, 2013). To this feature, we add the following characters of the caudal skeleton: caudal node formed by the caudal-most eighth and seventh centra; dorsoventrally depressed tail with short, well-separated and nonfused haemal processes; long caudal ribs and short neural spines with flattened dorsal top, forming a horizontal tail fin in life.

SKULL DESCRIPTION

Squamosals—The squamosals extend well posterior to the occipital condyle. The posterior extension of both squamosals under the pterygoids encloses the atlas-axis, constraining its lateral movement. Each squamosal covers the dorsal portion of the quadrate and forms an internal cavity for the adductor chamber (Fig. 2). The squamosals are broadly fused to the pterygoids through a craniocaudally oriented suture and together they form a bony shelf that ventrally encloses each temporal fossa. The squamosals of *Aristonectes quiriquinensis* have an unusual shape. Instead of forming a high squamosal arch as in most xenopsarians, they do not meet dorsally in the midline. The squamosals are shifted horizontally in a rostral direction, being anteriorly fused to the parietals and the basioccipital (Fig. 3), whereas the middle part of the squamosal extends posterior to the occipital condyle (together with the pterygoids). The posterior margin of the left squamosal is missing its dorsomedial surface; however, its posteromedial margin is well preserved. This confirms that the squamosal indeed forms the entire posterior margin of the temporal fenestra. The squamosal-pterygoid suture is as long as the

combined length of the atlas-axis and the braincase. On its posteromedial margin, each squamosal has a dorsal process that ends in a conspicuous additional ossification. The latter do not correlate with any posterior skull bone known in elasmosaurids and could belong to an ossified soft tissue. They are located well dorsal to paroccipital processes and do not appear to be derived from them.

Anteriorly, the squamosals extend to join the braincase under the exoccipital-opistothics on each side of the braincase. There is no evidence of a dorsal process of the squamosal near the occipital condyle; thus, the squamosals do not meet in the midline. This configuration radically differs from any elasmosaurid (and from any plesiosaur) where normally a squamosal arch is formed by the medial union of both squamosals in a position over the foramen magnum (Welles, 1943, 1952, 1962).

Pterygoids—The left pterygoid is the better preserved, whereas the right one is partially crushed. The pterygoids are large and project posteriorly away from the braincase, reaching caudally to the fourth cervical vertebra (Fig. 4). The posterior extension of both pterygoids encloses the atlas-axis, c3, and c4, leaving a reduced space between the cranium and vertebrae and constraining lateral movement at the craniovertebral joint. The pterygoids are mostly flat but slightly recurved dorsally in the mid-portion beside the braincase. Posteriorly, each narrows to a pterygoidal process that has a posterior contact with the quadrate as well as a long craniocaudal contact with the squamosal. The anterolateral portion is in contact with the palatines, whereas the contact with the ectopterygoid is narrow and restricted to its anterolateral margin. The pterygoid–squamosal contact is better preserved on the left. Ventrally, the squamosal has a mid-anterior process that enters into the pterygoid shelf, having a triangular suture line that is well fused and quite difficult to follow. The posterior interpterygoid vacuities, as assessed by O'Keefe (2001), are here considered as the palatal fossa that occurred in the posteroventral part of the skull, between the pterygoids, exposing the ventral surface of the braincase. Thus, the pterygoids enclose the interpterygoid vacuities except anteromedially, where a short section of the margin is formed by a lateral thickenning of the parasphenoid and an anteromedian extension of each pterygoid. Posteriorly, those vacuities are open because posteromedial contact between the pterygoids is lacking. The posterior shelf inside both vacuities is formed medially by the parasphenoid and laterally by the basioccipital.

The quadrate flange of the pterygoid is large, expanded laterally and caudally, and sutures broadly with the squamosal as well as the quadrate.

Among elasmosaurids, the pterygoids commonly meet both anterior and posterior to the posterior interpterygoid vacuities (O'Keefe, 2001), whereas in cryptoclidids such as *Tricleidus seeleyi* (O'Keefe, 2001:fig. 16) these do not meet, being medially interrupted by the parasphenoid. Some polycotylids exhibit a configuration resembling the condition in *Aristonectes quiriquinensis*, although there is a small contact of the pterygoids posterior to the posterior interpterygoid vacuities (O'Keefe, 2004:fig. 17),
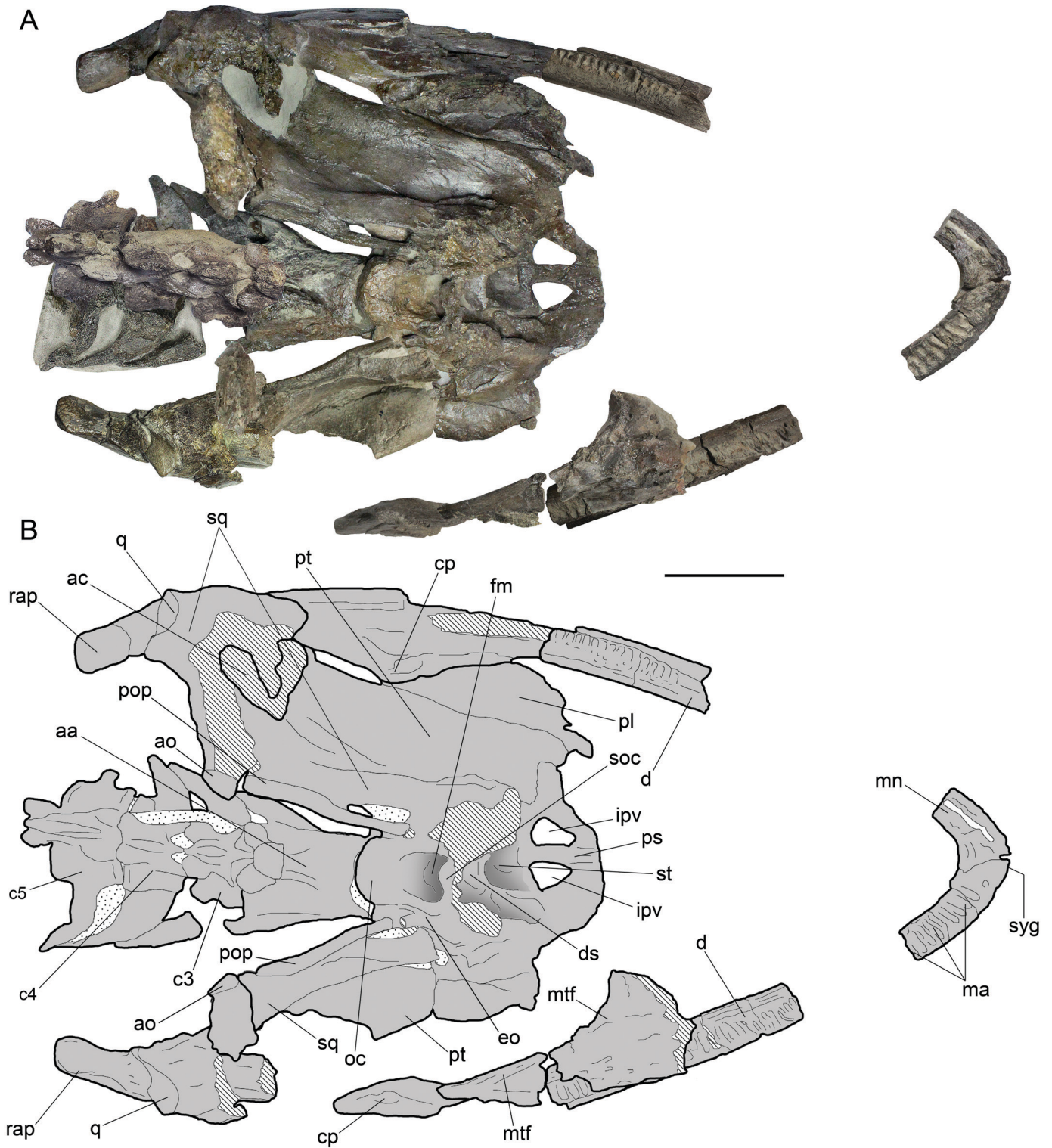
FIGURE 2. Skull of *Aristonectes quiriquinensis* (SGO.PV.957, holotype). **A**, dorsal view; **B**, scheme of the anatomical elements elements observed in dorsal view. **Abbreviations**: **aa**, atlas-axis; **ac**, adductor chamber; **an**, angular; **ao**, accessory ossification; **cp**, coronoid process; **c3**, third cervical vertebra; **c4**, fourth cervical vertebra; **c5**, fifth cervical vertebra; **d**, dentary; **ds**, dorsum sellae; **eo**, exoccipital-opisthotic; **fm**, foramen magnum; **ipv**, interptery-goid vacuities (functional internal choanae); **ma**, main alveoli; **mn**, cast of the mandibular nerve; **mtf**, margin of the temporal fenestra; **pl**, palatine; **pop**, paroccipital process; **pr**, prootic; **ps**, parasphenoid; **pt**, pterygoid; **q**, quadrate; **rap**, retroarticular process; **soc**, supraoccipital; **sp**, splenial; **sq**, squa-mosal; **st**, sella turcica; **syg**, symphyseal groove. Scale bar equals 100 mm.
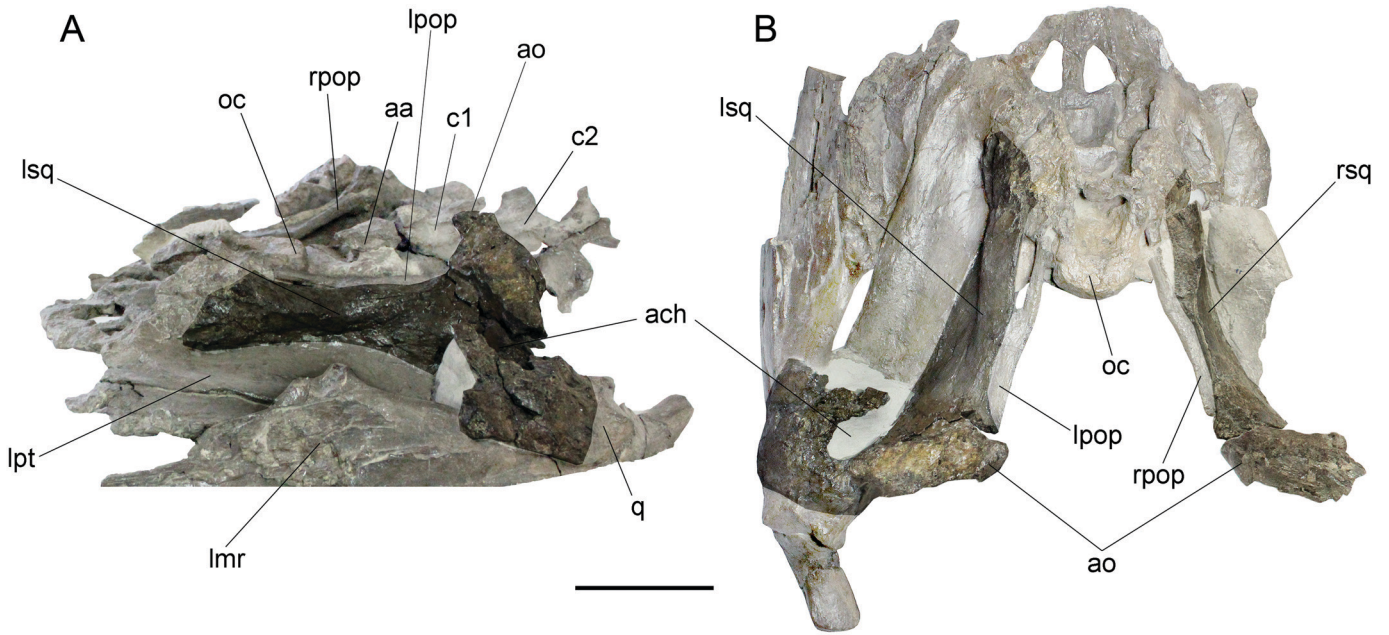
FIGURE 3. Squamosals of *Aristonectes quiriquinensis* (SGO.PV.957, holotype). **A**, left dorsolateral view of the posterior skull, showing the left squamosal; **B**, dorsal view of the posterior skull showing both squamosals. **Abbreviations**: **aa**, atlas-axis; **ach**, adductor chamber; **ao**, accessory ossification; **c1**, first cervical; **c2**, second cervical; **lmr**, left mandibular ramus; **lpop**, left paroccipital process; **lpt**, left pterygoid; **lsq**, left squamosal; **oc**, occipital condyle; **q**, quadrate; **rpop**, right paroccipital process; **rsq**, right squamosal. Scale bar equals 100 mm.
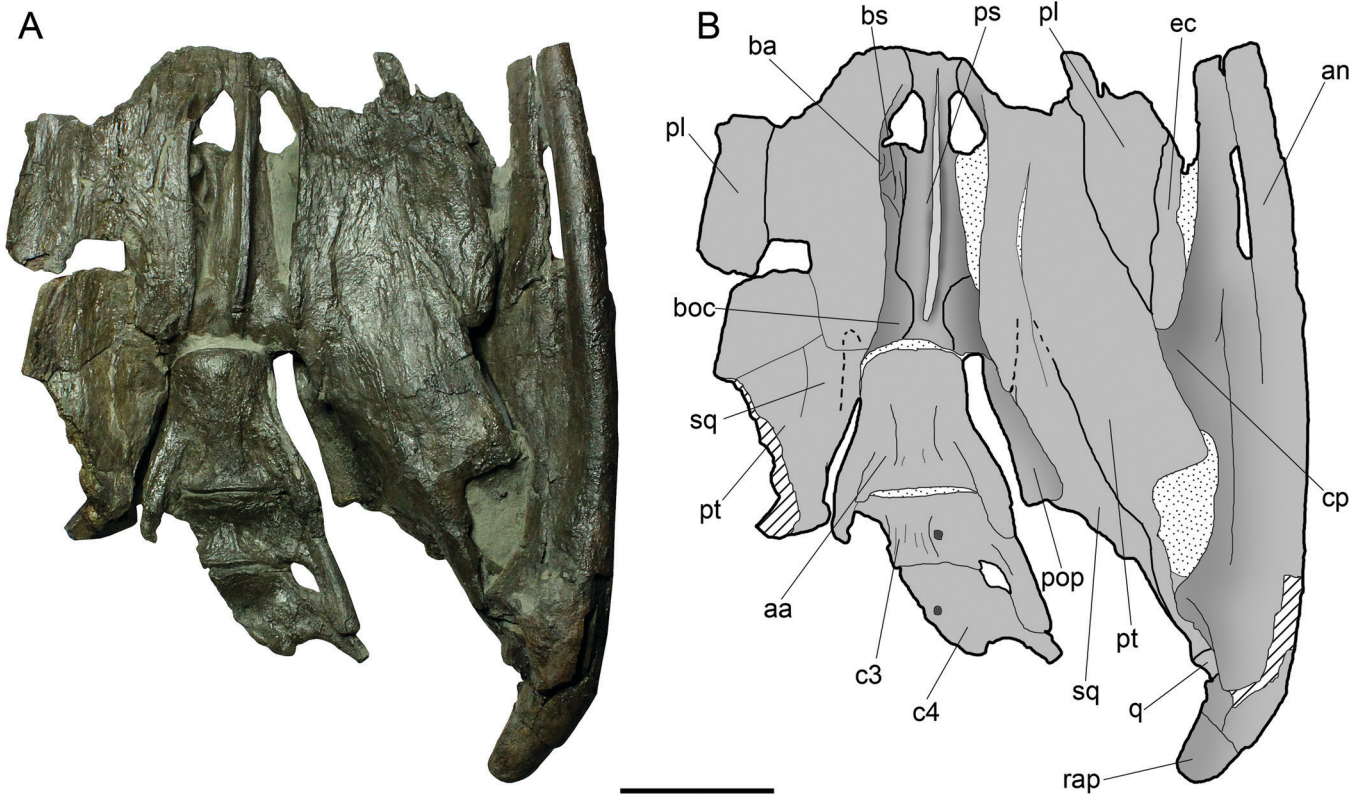

FIGURE 4. Skull of *Aristonectes quiriquinensis* (SGO.PV.957, holotype). **A**, ventral view; **B**, scheme of anatomical elements observed in ventral view. Dashed lines indicate obscured pterygoid–squamosal suture segments. **Abbreviations**: **aa**, atlas-axis; **an**, angular; **ba**, basal articulation; **boc**, basioccipital; **bs**, basisphenoid; **cp**, coronoid process; **c3**, third cervical vertebra; **c4**, fourth cervical vertebra; **ec**, ectopterygoid; **pl**, palatine; **pop**, paroccipital process; **pt**, pterygoid; **ps**, parasphenoid; **q**, quadrate; **rap**, retroarticular process; **sq**, squamosal. Scale bar equals 100 mm.
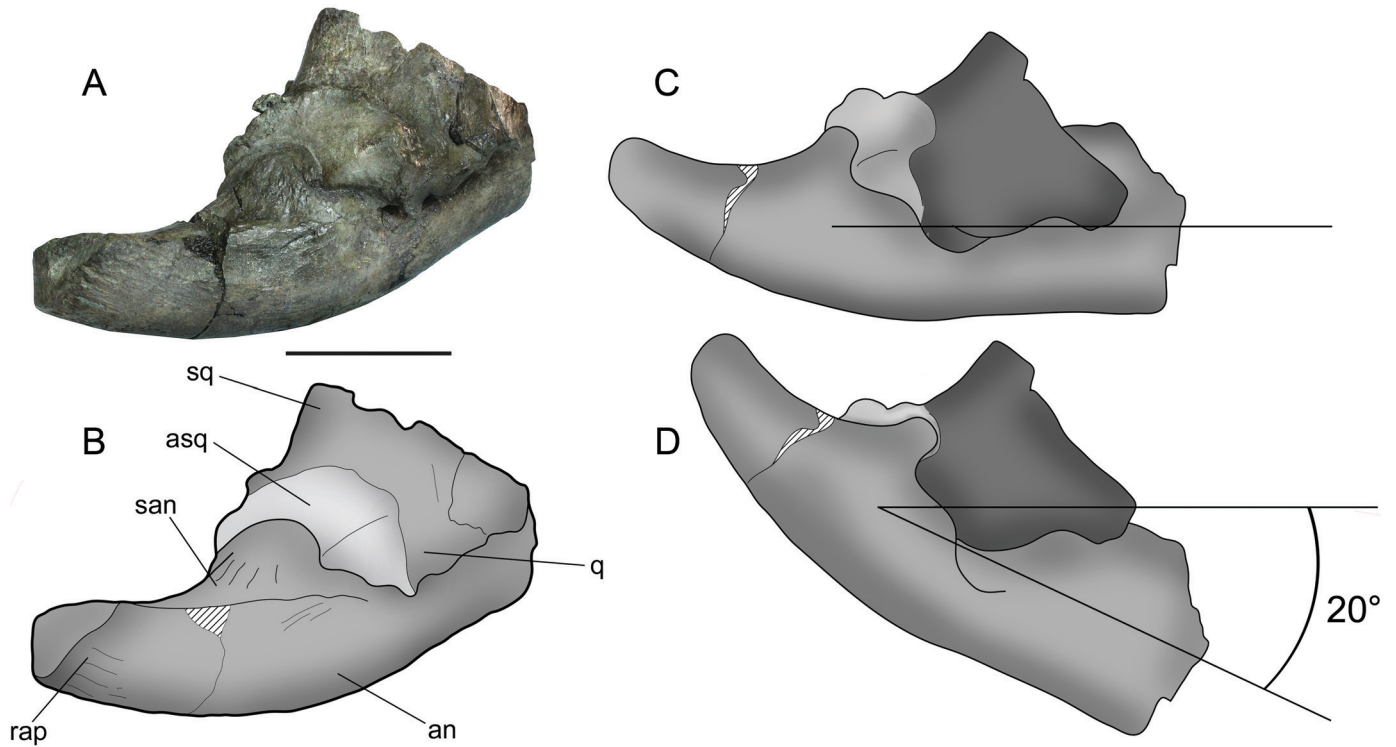
FIGURE 5. *Aristonectes quiriquinensis* (SGO.PV.957, holotype). **A**, right posterior ramus, showing the mandibular glenoid; **B**, interpretative diagram of the previous view; **C**, diagram of the right glenoid in external (right lateral) view, showing the ramus in occlusion as it is preserved on the fossil; **D**, diagram showing the expected maximum displacement of the ramus considering the length of the articular surface of the quadrate. This indicates a maximum mouth opening angle of ca. 20°. **Abbreviations**: **an**, angular; **asq**, articular surface of the quadrate; **q**, quadrate; **rap**, retroarticular process; **san**, surangular; **sq**, squamosal. Scale bar equals 50 mm.
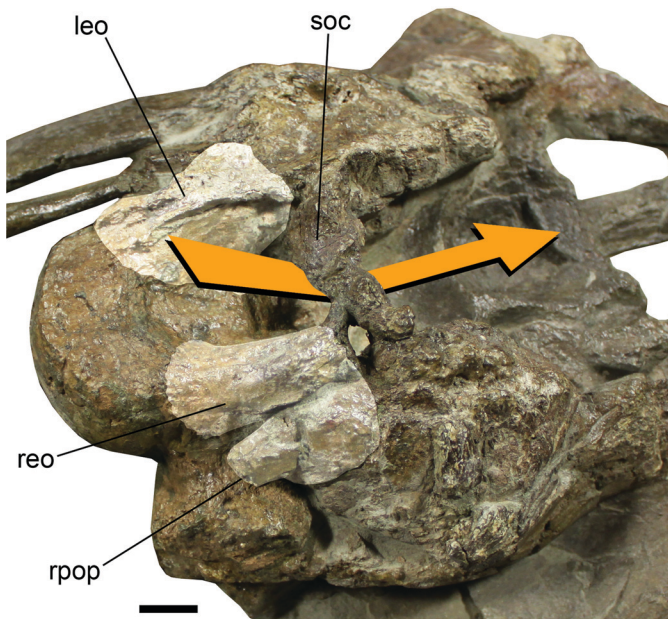

FIGURE 6. Right dorsolateral view of the braincase, showing the disposition of the exoccipital-opisthotics recurved rostrally and the angle of entrance of the spinal cord through the foramen magnum. **Abbreviations**: **leo**, left exoccipital-opisthotic; **reo**, right exoccipital-opisthotic; **rpop**, right paroccipital process; **soc**, supraoccipital. Scale bar equals 10 mm.

contrary to *Aristonectes quiriquinensis*, where the pterygoids do not meet posteriorly.

Quadrate—SGO.PV.957 has both quadrates, but they are largely obscured by the articulated squamosals and by the mandibular rami. Despite this, it is possible to observe the articular surface of the craniomandibular joint. This is diagonally oriented in dorsal view, with its external margin reaching more rostrally than the internal (lingual) margin. The articular surface of the quadrate is mediolaterally expanded. The dorsal part of the articular surface is consistent with the posterodorsal process of the surangular in the ramus glenoid (Fig. 5). This causes a restriction to the mouth opening, leaving between 25 and 30 mm of articular surface available for mandibular movement. This would have limited mandibular gape to about 20° with respect to the skull axis (Fig. 5).

Exoccipital-Opisthotics—These elements are 20% taller dorsoventrally than mediolaterally broad. No nerve foramina are visible. The right exoccipital-opisthotic is the better preserved, showing the suture with the basioccipital, which is just rostral to the constriction at the base of the occipital condyle. Both exoccipital-opisthotics, which are crushed to a degree that is hard to measure, contact the basioccipital through a diagonal suture (Fig. 6). The proximal end of each paroccipital process is ventrally oriented, whereas the posterior (distal) end of the paroccipital process reaches the dorsal-most portion of the squamosals (see below). This condition indicates that the degree of deformation of the basioccipital and exoccipital-opisthotics is not drastic and that there is pronounced rostral shear of the dorsal aspect of the occipital arch, resulting in a foramen magnum with an oblique angle to the vertical axis. A very
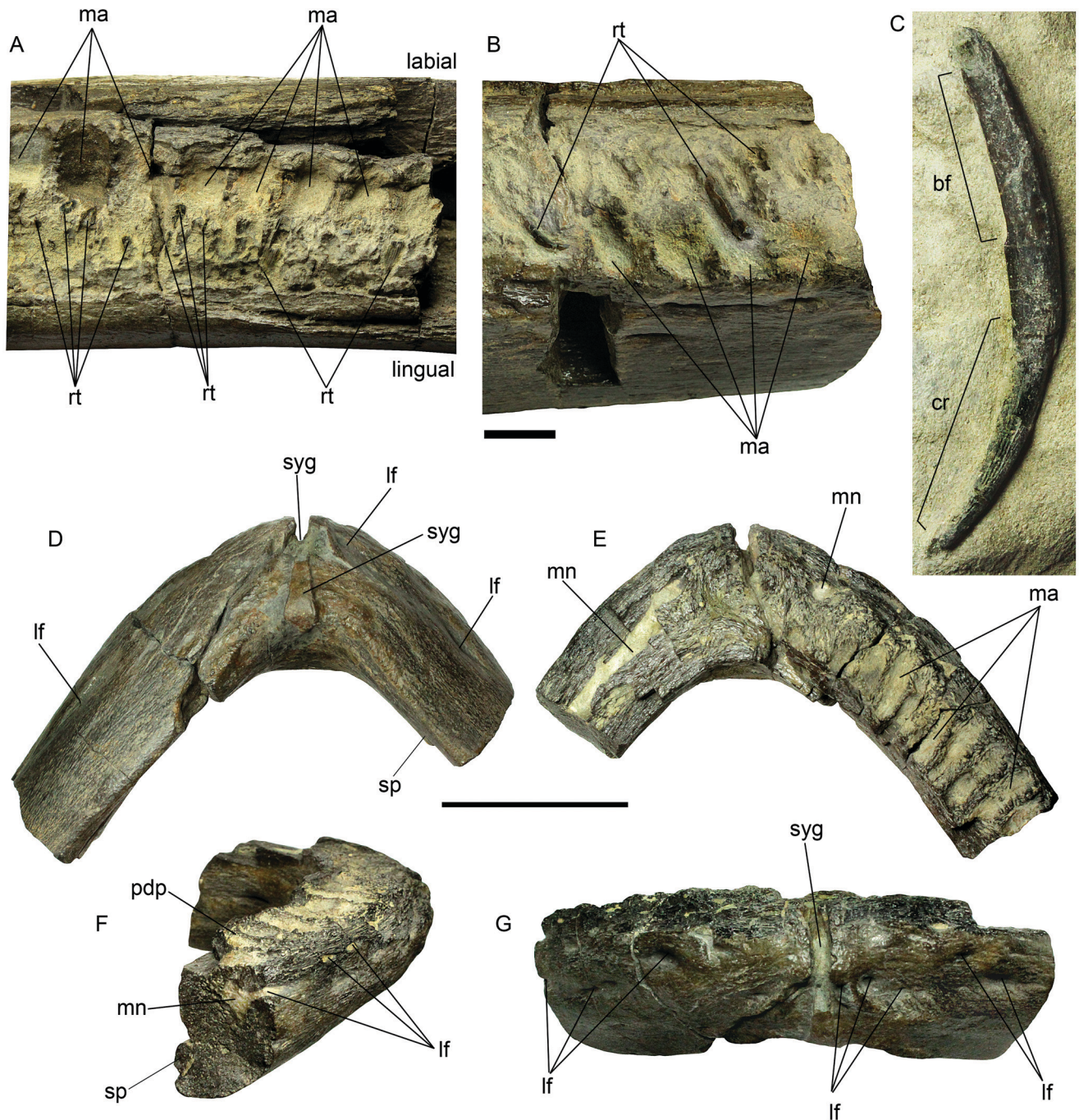
FIGURE 7. Mandibular features of *Aristonectes quiriquinensis*. **A**, dorsal (occlusal) view of the left dentary portion; **B**, dorsolateral view of the right dentary portion; **C**, complete tooth in profile view; **D**, symphyseal portion of the mandible in ventral view; **E**, dorsal view; **F**, right lateral view; **G**, anterior view. **Abbreviations**: **bf**, basal facet for the replacement tooth; **cr**, tooth crown; **fa**, functional alveoli; **lf**, labial foramina; **ma**, main alveoli; **mn**, mandibular nerve; **rt**, replacement teeth; **sp**, splenial; **syg**, symphyseal groove. Scale bars equal 10 mm (**A–C**) and 50 mm (**D–G**).

similar anatomical feature also occurs in *Alexandronectes zealandiensis* (Otero et al., 2016:fig. 2a, b).

Paroccipital Processes—These elements are very long and slender. They extend from the exoccipital-opisthotics, having a circular cross-section that becomes oval in the mid-portion of each process. Unlike most elasmosaurids, the paroccipital processes of *Aristonectes quiriquinensis* are almost horizontal and oriented posteriorly. Approximately 40% of each process is craniocaudally oriented, whereas the remaining 60% is slightly bent and articulates laterally with the squamosals along the rest of the

shaft. The most posterior end of each paraccipital process overlies the most dorsal part of each squamosal.

Basioccipital—The general shape of the basioccipital is difficult to observe because all surrounding elements remain articulated and cover most of it. Its width is nearly twice the breadth of the occipital condyle. The articulation usually regarded as the pterygoid facet can be seen in right lateral view, although in this specimen the articulation largely involves the squamosal. In ventral view, the basioccipital can be observed as partially covered
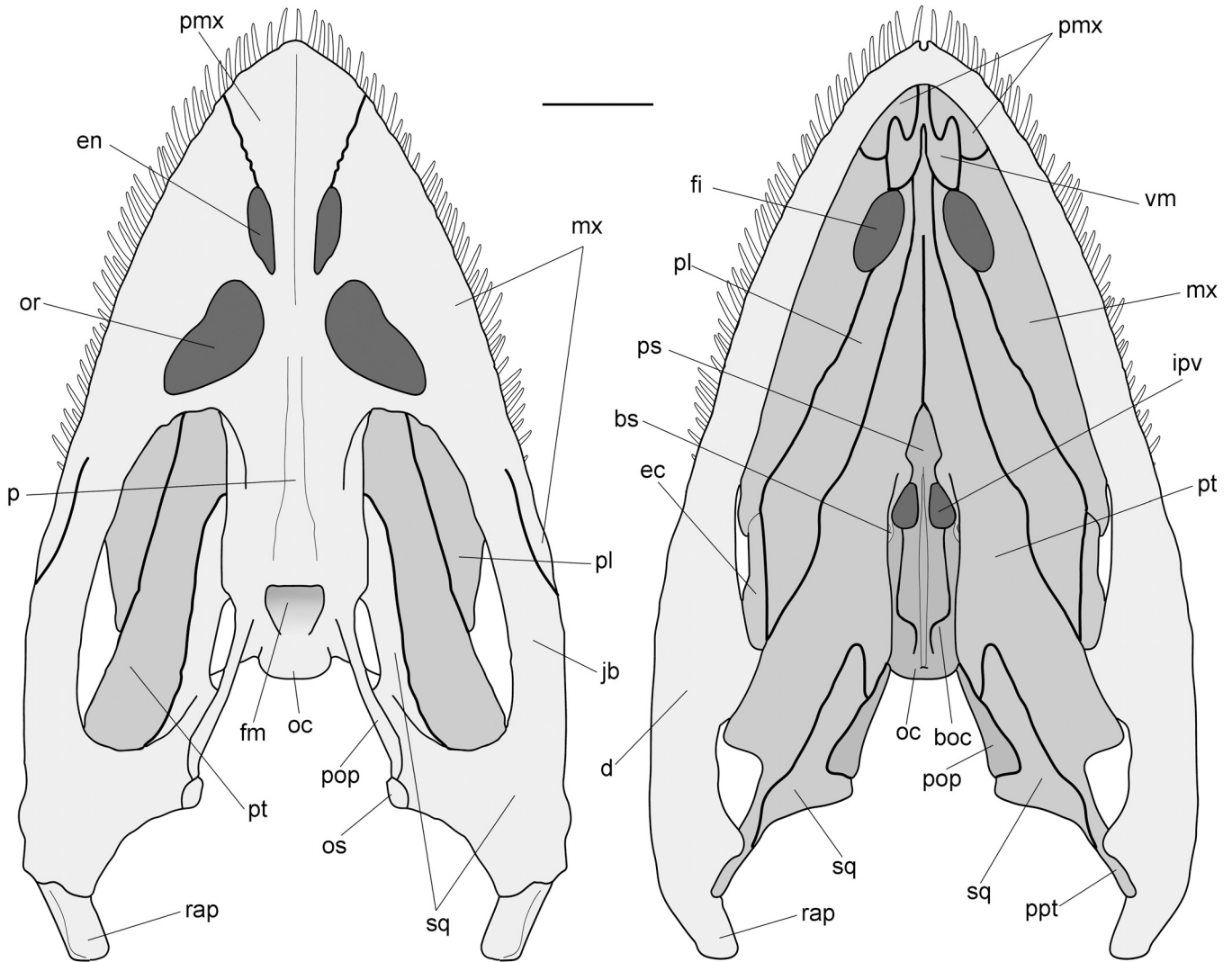
FIGURE 8. Reconstructed skull of *Aristonectes quiriquinensis*. Interpretation based on the preserved portions of the holotype SGO.PV.957. Missing portions are added based on the holotype of *Aristonectes parvidens*. Orbits and external nares are based on TTU P9219, holotype of '*Morturneria*' *seymourensis*, the closest relative preserving those portions. **Abbreviations**: **ao**, accessory ossification; **boc**, basioccipital; **bs**, basisphenoid; **d**, dentary; **ec**, ectopterygoid; **en**, external naris; **fi**, foramen insicivum; **fm**, foramen magnum; **ipv**, interpterygoid vacuities (functional internal choanae); **jb**, jugal bar; **mx**, maxilla; **oc**, occipital condyle; **or**, orbit; **p**, parietal; **pl**, palatine; **pmx**, premaxilla; **pop**, paroccipital process; **ppt**, posterior process of pterygoid; **ps**, parasphenoid; **pt**, pterygoid; **rap**, retroarticular process; **sq**, squamosal; **vm**, vomer. Scale bar equals 100 mm.

in the midline by the parasphenoid. Both elements form the internal surface of the interpterygoid vacuities.

Basisphenoid—Only the right anteroventral portion bearing the basal articulation can be observed. The latter is surrounded by few folds, possibly representing the location of the internal carotid artery, although the internal carotid foramen is not visible. The contact with the basioccipital is not visible because of the ventral extension of the parasphenoid.

Parasphenoid—The long, low parasphenoid ventrally covers the basioccipital and the basisphenoid for two thirds of its length, whereas its remaining third extends rostrally. The anterior portion inserts between the pterygoids. It bears a ventral keel that separates the interpterygoid vacuities. The basisphenoid extends anteriorly to the braincase, being rostrally surpassed by a small part of the interpterygoid vacuities, which have a triangular opening. The ventral keel of the parasphenoid is anteriorly sharp and broadens posteriorly, fading into a rounded and soft surface in its posterior margin. The sutures of the parasphenoid with the

elements of the braincase are visible, being relatively parallel to the anteroposterior axis and becoming constricted and concave over the basioccipital.

Ectopterygoids—The ectopterygoids are best seen in ventral view. Each forms an extensive contact with the palatine and posteriorly contacts the pterygoid. The dorsal extensions cannot be evaluated because they are covered by other elements.

Palatine—The left palatine is the better preserved, although it is incomplete. The element displays a general triangular outline pointing posteriorly; the preserved portion is flat, with no observable dorsal projection.

Supraoccipital—A small fragment of the supraoccipital is preserved, enclosing the foramen magnum dorsally. Its relationship with other elements cannot be ascertained because of its incompleteness.

Dentition—Examination of the alveoli on the dentary shows that the teeth projected dorsolaterally in the posterior portion of the jaw and gradually transitioned to an almost horizontal orientation
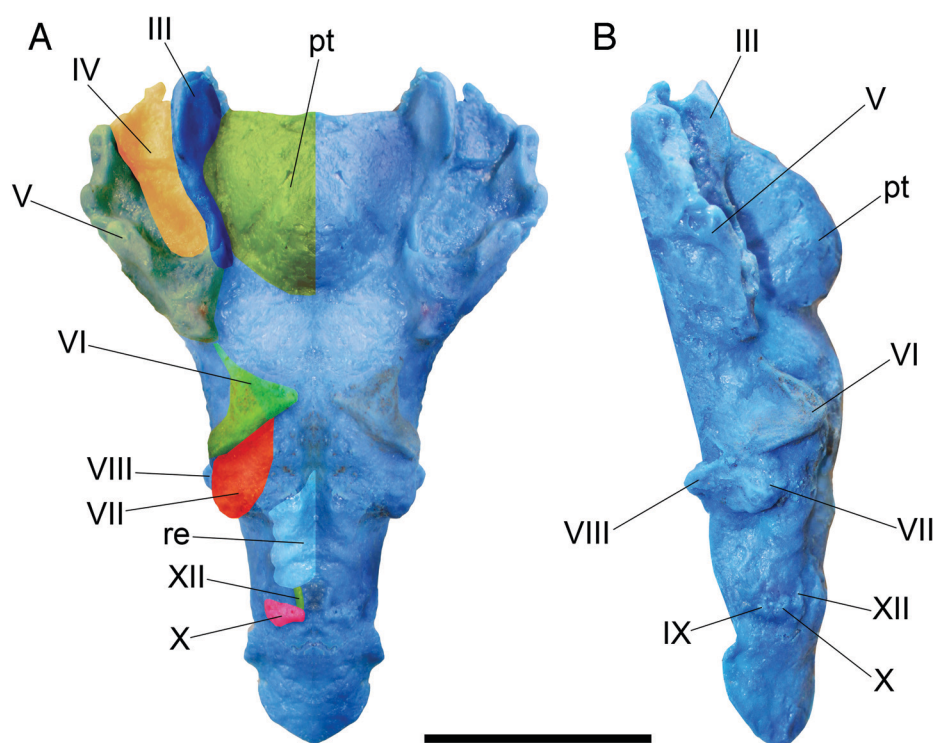
FIGURE 9. Internal cast of the braincase. **A**, inferior view of braincase cast reconstructed by mirroring of the better preserved right side; **B**, right lateral view of the braincase cast. **Abbreviations**: **III**, nervus oculomotorius; **IV**, nervus trochlearis; **V**, nervus trigeminus; **VI**, nervus abducens; **VII**, nervus facialis; **VIII**, nervus vestibulocochlearis; **IX**, nervus glossopharyngeus; **X**, nervus vagus; **XII**, nervus hypoglossum; **pt**, pituitary; **re**, rombencephalon; **su**, sulci. Scale bar equals 50 mm.

in the anterior part of each dentary. Dorsal to the teeth and occlusally disposed, there are small horizontal alveoli-like structures that are irregular in shape and distribution. Few of these structures still preserve the replacement tooth. All of those teeth are oriented horizontally (Fig. 7A). The best preserved replacement teeth (Fig. 7B) bear lingual striations. The labial surfaces are only visible on two teeth from the right dentary, and both show smooth enamel. Interestingly, all of the replacement teeth are horizontal but have their crowns oriented rostrally. This is consistent with the general shape of the isolated functional teeth recovered during the preparation (Fig. 7C), indicating that the teeth were oriented in a combined occlusal–anterior direction.

Mandibular Symphysis—A deep symphyseal pit present in the anterior joint of both jaw rami extends from the midline to the ventral margin of the symphysis. Ventrally, it is surrounded by two delicate keels (Fig. 7D–G) that have been interpreted previously as representing a mental boss (Otero et al., 2014c). The symphyseal pit is consistent with the anterior placement of the geniohyoid muscle, and its depth suggests a strong attachment of the latter.

Reconstruction of the Skull of *Aristonectes quiriquinensis*

The rostral portion of the skull of *Aristonectes quiriquinensis* is missing; however, its length can be estimated based on the available dentary portions and the symphysis. In addition, the right dentary was crushed together with a skull fragment preserving the anterior margin of the temporal fossa. The left dentary is preserved in two continuous parts and the posterior part remains in anatomical position with respect to the skull. All of these elements make it possible to estimate a general skull outline and its length. The temporal fossae are large, representing over 35% of the skull length between the symphysis and the retroarticular process. The preserved portions indicate that both orbits and the external nares were restricted to the anterior third of the skull. Integration of these observations with the preserved portions allows us to propose a tentative reconstruction of the skull

(Fig. 8). Unknown portions, mostly the orbits and external naris, are based on the preserved elements of *Aristonectes parvidens* as well as its hypothesized sister taxon TTU P9219 (Chatterjee and Small, 1989). The large temporal fossae reflect a greatly enlarged posterior margin of the skull. Interestingly, the relative placement of the orbits and external naris is similar to that in non-aristonectine elasmosaurids, suggesting that the dorsolateral orientation of the orbits could be related to the lateral broadening and dorsoventral flattening of the *Aristonectes* skull but retaining a plesiomorphic position common in elasmosaurids. Moreover, the braincase retains a plesiomorphic shape with respect to the orbits and external naris, whereas the mandibular articulation is dramatically shifted caudally with respect to non-aristonectine elasmosaurids (linked to the pterygoid/squamosal posterior extension).

Neuroanatomy

Pituitary—The largest concave structure observed in the mesencephalic region is the cast of the sella turcica, which reflects a large pituitary gland (Fig. 9). That structure has a slightly broader and ventrally flat anterior portion with a maximum width of ca. 45 mm, whereas its anterior margin has a deep sulcus and its posterior end is ventrally rounded and deep. Over the left lateral portion of the cast (which reflects the better preserved right side of the braincase), two sulci can be distinguished. These are here tentatively interpreted as the boundaries between the pars tuberalis, the pars intermedia, and the pars nervosa. Based on these sulci, the pars tuberalis should be the largest, whereas the pars intermedia appears as a smaller structure more visible laterally. The pars nervosa appears to be small and restricted to the posterior margin of the infundibular space. The combined size of the structures interpreted as pars intermedia and the pars nervosa is even smaller than the putative pars tuberalis.

Cranial Nerves—Identification of these elements follows Ten Donkelaar (1998:figs. 20.7–20.10). Except for the pair XI, there is visible evidence of the cranial pairs iii to XII on the silicon cast

(Fig. 9). Lateral to the infundibulum, a large nerve cast is antero-posteriorly extended. This is interpreted as the nervus oculomotorius (III). The latter is reflected in the skull as a deep sulcus that is parallel to the sella turcica. A second deep sulcus in the external margin of the braincase at the position of the pituitary is interpreted as the nervus trigeminus (V). Between iii and v, there is a shallow, broad sulcus interpreted as the nervus trochlearis (IV). The medulla oblongata is slightly larger and laterally narrower than the infundibulum cast. Over the former, there is a large, triangular nervous root, posteriorly followed by a second bulky root. These are interpreted as the nervus abducens (VI) and nervus facialis (VII), respectively. Dorsal to vii, there is a small, bulky root interpreted as the nervus vestibulocochlearis (VIII; = nervus statoacusticus in Ten Donkelaar, 1998). In the mid-ventral portion, the rhombencephalon is well marked. This is posteriorly followed by an 'L'-shaped structure split in two nervous roots, one being small, anteroposteriorly oriented, and interpreted as the nervus hypoglossum (XII), whereas the second, mesolaterally oriented, is interpreted as the nervus vagus (X). The position of the nervus accessorius (XI) remains uncertain due to the preservation of the skull.

Labial Foramina—As in many plesiosaurs, several deep oval foramina are present in the symphyseal end of the dentaries. These are set between the ventral surface of the dentary (which is a very compact tissue) and below the paradental plate where the alveoli reside. These foramina are craniocaudally elongate (6 mm broad, 1 mm high). The left side of the symphysis displays an internal canal visible in dorsal view because part the paradental plate is absent (Otero et al., 2014c:fig. 8a). This canal is rounded and broad (6 mm diameter in cross-section) and represents the anterior extension of the mandibular nerve running in the Meckelian canal. The latter is in direct contact with the labial foramina distributed along the symphyseal portion.

DESCRIPTION OF NEW POSTCRANIAL FEATURES

Atlas-Axis and Anterior-most Cervical Vertebrae—The atlantal cup is unusual among elasmosaurids, bearing a rostrally projected anteroventral margin. Such a projection restricts the ventral movement of the skull with respect to the atlas-axis, causing a blockage. In addition, the atlas-axis ribs are in contact with the ribs of the third cervical vertebra, and the atlas-axis complex is laterally surrounded by the squamosal–pterygoid shelf, precluding its lateral movement. Ribs of the third cervical vertebra are also in contact with the ribs of the fourth cervical vertebra. All of these features show that the anterior-most neck elements had reduced movement possibilities.

Elongated Extremities—*Aristonectes quiriquinensis* has very long extremities. The right forelimb (which is the most complete) measures ca. 3 m from the humeral head to the distal-most preserved phalanx. The pectoral girdle has an interglenoid breadth of 1 m, resulting in a lateral wingspan of at least 7 m. Combining the neck length (3.5 m), the estimated trunk length (4 m), and the tail length extrapolated from the juvenile specimen SGO.PV.260 suggests a body length of over 10 m. Therefore, each front limb is equivalent to nearly one third of the total body length. Similar proportions are present in the pectoral flippers of the extant humpback whale (*Megaptera novaeangliae*). Interestingly, no other extant or known fossil cetacean has such proportions in its pectoral flippers. Among plesiosaurs, such forelimb/trunk proportions are found in the Toarcian rhomaleosaurid *Meyerasaurus victor* (Fraas, 1910; Smith and Vincent, 2010). The current proportions in *Aristonectes quiriquinensis* seem to be the first known occurrence of such a feature among elasmosaurids.

General Body Shape—The trunk of the holotype of *Aristonectes quiriquinensis* was found partially disarticulated, whereas in the referred juvenile specimen SGO.PV.260 these same elements are articulated. This was used as basis for a more accurate interpretation of the trunk shape. The maximum length of the coracoid is about half the length of the articulated gastralia and almost the same as the combined length of the pubis and ischium. By placing all of these portions in anatomical position (Fig. 10), they show a trunk that is comparatively more slender than in other plesiosaurs where the trunk proportions are well known. In *Cryptoclidus*, the trunk is massive and thick with respect to the rest of the axial skeleton (Andrews, 1910) and the craniocaudal length of the gastral basket is shorter than each girdle. In contrast, the trunk is dorsoventrally compressed in *Tatenectes* (O'Keefe et al., 2011). The proportions of SGO.PV.260 are more similar to those observed in *Plesiosaurus dolichodeirus* (Storrs, 1997) and in the trunk of elasmosaurids such as *Hydrotherosaurus alexandrae* (Welles, 1943). The approximately 43 cervical vertebrae, the thick and dorsoventrally tall neck, together with the new notion of the skull proportions obtained here, adds to the reconstruction of the general body shape of *Aristonectes quiriquinensis*.

Tail—The tail of *Aristonectes quiriquinensis* (Fig. 11) is known by the referred juvenile specimen SGO.PV.260. It includes 35 centra, all of which are broader than tall or long (Fig. 11A–D), having distinctive octagonal articular facets determined by the large, lateral rib facets and a large pair of neural pedicels, as well as a flat ventral surface. Neural spines became shorter and blunt, acquiring a thick dorsal top with a flat surface, suggesting the existence of a strong ligament along the dorsal extension of the tail. The caudal ribs have shafts that are longer than the centrum breadth. Their articular facets are large and oval, occupying nearly the whole centrum length. Medially, each rib shaft is recurved posteriorly and has a distal anteroposterior thickening. Distally, each caudal rib end has a dorsoventrally flattened section. The distal end of each caudal rib of the referred specimen SGO.PV.260 has an articular surface for a cartilaginous extension, indicating that the lateral extension of the tail was even broader in life. Finally, the hemal processes are massive, very short, recurved medially, and do not meet in the midline, being instead well separated. Thus, a hemal arch is not formed in the caudal-most portion.

A node consisting of two relatively anteroposteriorly shortened vertebrae occurs between the eighth and seventh caudal-most centra (i.e., 27th and 28th caudal vertebrae). This node is similar to that described by Smith (2013) for *Rhomaleosaurus zetlandicus*. The dorso-caudal asymmetry observed in the centra has been interpreted as a possible subtle ventral displacement of the last caudal centra, associated to a vertical tailfin as occurs in thalattosuchians, mosasaurs, and ichthyosaurs (Smith [2013] and references therein). In the case of SGO.PV.260, the centra involved in the node do not have dorso-caudal asymmetry; instead, they possess a straight articular facet that precludes any ventral (or dorsal) displacement of the caudal-most complex. Additionally, the already short and massive hemal processes become even shorter starting from the node to the caudal end. Finally, the neural spines do not reflect any structural change that could indicate mobility for the caudal-most elements, as occurs in at least some cryptoclidians that have dorsally enlarged caudal-most neural spines (Wilhelm and O'Keefe, 2010).

The caudal elements in the juvenile specimen SGO.PV.260 are broader than tall and taller than long, suggesting the presence of a dorsoventrally compressed and laterally expanded tail. The low neural spines with a dorsal flat surface suggest the existence of a strong ligament helpful for vertical movement. In addition, the large caudal ribs are dorsoventrally compressed and have distal facets for cartilaginous extensions, indicating an even broader section than that represented by the osteological material alone. Additionally, the nonfused and well-separated hemal processes add to the
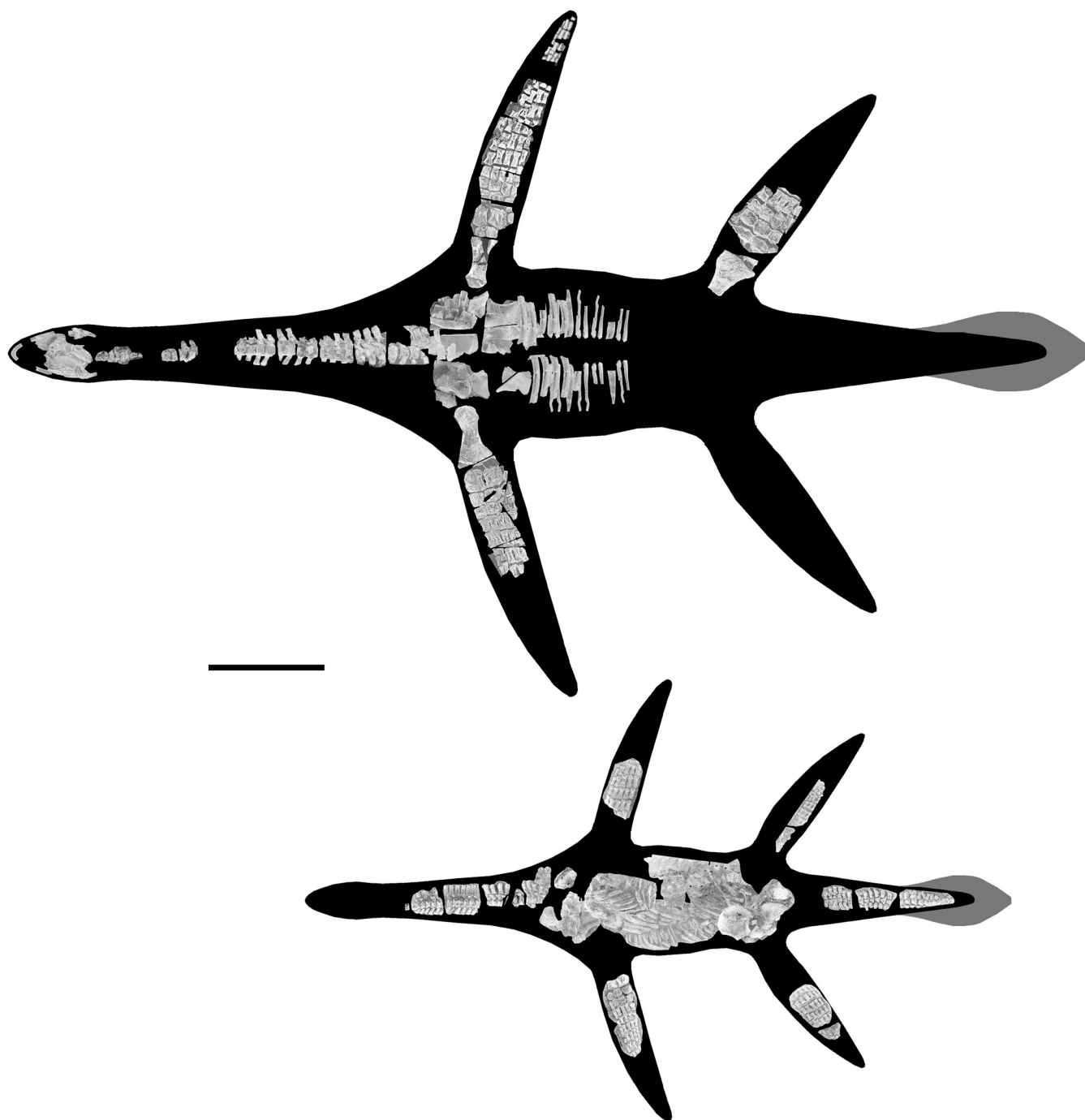
FIGURE 10. General body shape of *Aristonectes quiriquinensis*. Estimated outline of the body based on a composite of the holotype (SGO.PV.957) and the most complete referred specimen (SGO.PV.260), below. Scale bar equals 1 m.

possibility of a vertical movement of the tail of SGO.PV.260, due to the absence of ventrally oriented chevrons.

The osteological features of the *Aristonectes quiriquinensis* caudal axial skeleton can be compared to those of sirenians, especially the genus *Trichechus*. In the latter, there are also large caudal ribs, short neural spines, as well as unfused hemal processes, depending on the ontogenetic stage (Buchholtz et al., 2007). Interestingly, all of these morphological features are related to a vertical motion of the tail. Moreover, in all of the species in the genus *Trichechus* there is a horizontal caudal fin.

DISCUSSION

Phylogenetic Analysis—Analysis with traditional search (Wagner trees, 1,000 replicates; 1,000 trees to save per replication) recovered over 5,000 trees, with some replications overflowing (Supplementary Data 2). This analysis returned a few unstable taxa within the Elasmosauridae. These taxa, Speeton Clay Plesiosaurian (NHMUK R8623) and GWWU A3B2, were previously recognized as 'wildcards' (Benson and Druckenmiller, 2014) and removed from subsequent analyses.
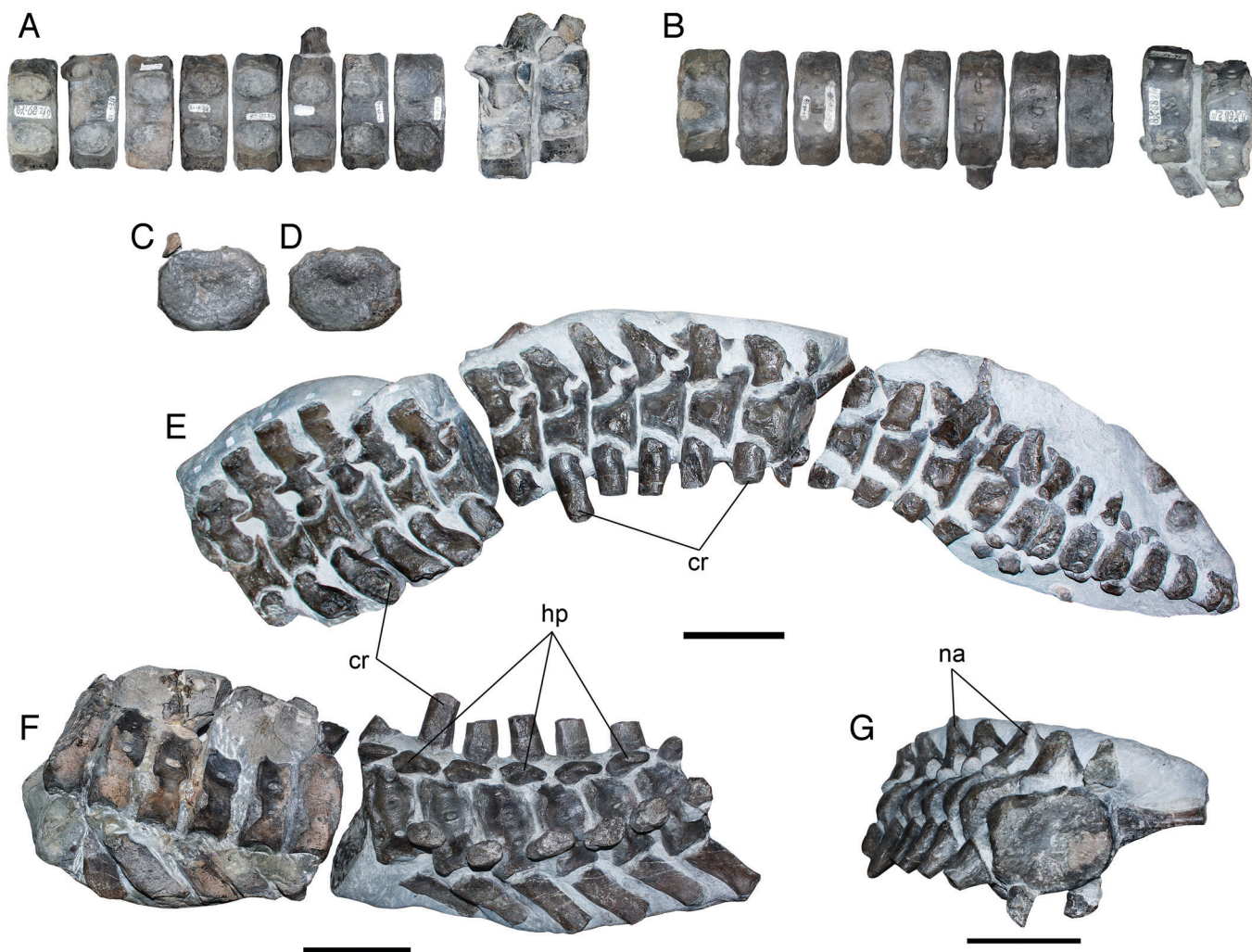
FIGURE 11. Caudal vertebrae of *Aristonectes quiriquinensis*. **A**, SGO.PV.94, anterior caudal series in dorsal view; **B**, same in ventral view; **C**, **D**, articular views of representative caudal centra of SGO.PV.94; **E**, SGO.PV.260, caudal-most portion in left lateral view, preserved in three blocks; **F**, two anterior blocks of the same specimen, in ventral view; **G**, same in anterior articular view. **Abbreviations**: **cr**; caudal ribs; **hp**, hemal processes; **na**, neural arches. Scale bars equals 100 mm.

In particular, GWWU A3B2 has been recently found to be conspecific with *Brancasaurus brancai* (Sachs et al., 2016). Therefore, it was pruned, leaving the holotype of *B. brancai* for analysis because the latter is a much more complete specimen. Bootstrap resampling of the new data matrix (2,000 replicates, standard sampling) recovered a cladogram (length = 1,745 steps; consistency index = 0.24; retention index = 0.61), with 86% support for the Aristonectinae (Supplementary Data 2). However, a large polytomy was recovered among basal plesiosaurians. A hypothesis of relationships of the Elasmosauridae and their sister taxa is proposed, based on these analyses (Fig. 12).

New Apomorphies of the Aristonectinae—Complete preparation of the skull of *Aristonectes quiriquinensis* allows close comparisons with other Weddellian elasmosaurids preserving a skull. These taxa are represented by *Aristonectes parvidens* Cabrera, 1941 from the upper Maastrichtian of Chubut, Argentina; TTU P9219 (Chatterjee and Small, 1989) from the upper Maastrichtian of Seymour Island, Antarctica; *Kaiwhekea katiki* Cruickshank and Fordyce, 2002 from the lower Maastrichtian of Shag Point, New Zealand; *Tuarangisaurus keyesi* Wiffen and Moisley, 1986 from Maastrichtian beds of Mangahouanga Stream, New

Zealand, and *Alexandronectes zealandiensis* (Hiller and Mannering, 2004; Otero et al., 2016). The presence of a large, posteriorly extended pterygoid–squamosal table is only known in TTU P9219 (O'Keefe et al., 2017), although this was not noted in detail in the original description (Chatterjee and Small, 1989). The presence of a similar condition cannot be verified in *K. katiki* due to its preservation; however, the distance between the occipital condyle and the mandibular glenoid is similar to that in *Aristonectes quiriquinensis*, suggesting the existence of a comparable skull extension posterior to the condyle. *Alexandronectes zealandiensis* indeed has a similar condition, with a more incipient posterior extension. Interestingly, the latter has an early Maastrichtian age, whereas *Aristonectes quiriquinensis* and '*Morturneria*' *seymourensis* are late Maastrichtian in age. Based on these observations, we propose the presence of a posteriorly extended pterygoid–squamosal plate as a potential synapomorphy of Aristonectinae.

Aristonectes quiriquinensis features an entrance of the foramen magnum with a comparatively low angle (ca. 60°) compared to most elasmosaurids (which are close to 90°). The same occurs in '*Morturneria*' *seymourensis* (O'Keefe et al., 2017) and in *Alexandronectes zealandiensis* and is also probably present in *K.*
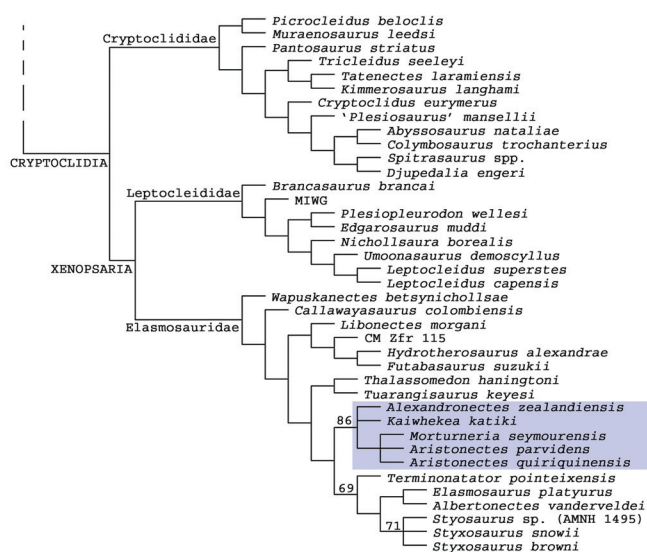
FIGURE 12. Cladogram of the Cryptoclidia extracted from the strict consensus cladogram (four MPCs, 1,522 steps, retention index = 0.66, consistency index = 0.27; see Supplementary Data 2). Bootstrap values over 50% are indicated in each respective branch. Aristonectinae (light blue square) had a bootstrap value of 86%.

katiki based on the exposed elements of the braincase, which are visible in left lateral view and are slightly angled rostrally (R.A. O., pers. observ., 2013). In addition, the anterior 'A'-shaped midline notch of the squamosal observed in dorsal view is a feature also present in *K. katiki* and *Alexandronectes zealandiensis*, whereas in *Aristonectes quiriquinensis* such a condition appears as more derived, with the squamosals completely separated on the midline and incorporated on each side of the braincase. In 'Morturneria' seymourensis, the squamosals are described as meeting in the dorsal midline, but the actual three-dimensional relationships of the squamosal with the rest of the skull are hard to assess from the original description (Chatterjee and Small, 1989) and are in the process of being redescribed (O'Keefe et al., 2017).

Another novel feature here found to be shared at least between 'Morturneria' seymourensis and *Aristonectes quiriquinensis* is the occurrence of replacement teeth of the dentary inside an almost horizontal chamber and disposed in a lateral position with respect to the main alveoli (Chatterjee and Small, 1989). In addition, both taxa have alveoli of the functional teeth that are horizontally oriented. This condition seems to be absent in *Kaiwhekea katiki* because the teeth, though small, are interlocked and are almost vertically oriented between the dentaries and maxillae (R.A.O., pers. observ., 2013). This is the plesiomorphic condition among elasmosaurids. Finally, a shared feature of the skull of *Aristonectes quiriquinensis*, TTU P9219, and the skull of *Alexandronectes zealandiensis* is the presence of pterygoids that do not meet posterior to the interpterygoid vacuities, being separated by the basioccipital/parasphenoid complex.

New Diagnostic Features of *Aristonectes quiriquinensis*—New skeletal morphologies of *Aristonectes quiriquinensis* that are found to be unique include: squamosals and pterygoids with an extensive contact (having an approximate length equivalent to the combined length of the atlas-axis and the braincase) forming a squamosal–pterygoid plate that extends posteriorly beyond the occipital condyle, reaching even the c4 centrum; squamosals do not meet dorsally in the midline over the foramen magnum, being instead extended laterally to the braincase; a very long and slender paroccipital process that is horizontally

oriented, with the distal half of the shaft fused to the squamosals; pterygoids that do not meet posterior to the interpterygoid vacuities; a structure equivalent to the posterior pterygoid process that is instead composed of the squamosal and the pterygoid. Ventrally, the quadrate of *Aristonectes quiriquinensis* contacts mostly with the squamosal, whereas the pterygoid has a small posterior process that barely contacts the quadrate; mandibular symphysis having a ventral chamber (symphyseal pit) and a groove for a strong attachment of the geniohyoid muscle; posterior end of the posterior interpterygoid vacuities extended until the contact surface with the atlas-axis and being dorsally recurved and having a soft surface; anteroventral margin of the atlantal cup rostrally extends beyond the dorsal surface, blocking a ventral bending of the head with respect to the neck; dorsoventrally compressed tail with very long caudal ribs and short, well-separated and thick hemal arches without midline fusion and not forming chevrons.

Osteological Modifications of the Skull—The skull possesses an unusual projection of the posterior mandibular rami and squamosals, with respect to the occipital condyle. This is a feature observed in very few elasmosaurids. Among latest Cretaceous taxa, at least four known specimens (other than the *Aristonectes quiriquinensis* holotype) have this condition: *Alexandronectes zealandiensis* from the Maastrichtian of New Zealand; *Kaiwhekea katiki* from the lower Maastrichtian of Shag Point, New Zealand, likely has a similar condition based on the relative position of the basioccipital with respect to the mandibular glenoid (R.A.O., pers. observ., 2013); *Zarafasaura oceanis* Vincent et al. (2011) from the upper Maastrichtian of Morocco, which is known by its holotype (isolated skull and mandible); and finally, another specimen referred to *Z. oceanis* including fragmentary skull and postcranial remains (Lomax and Wahl, 2013). The reconstructed mount of the head of the latter specimen (Lomax and Wahl, 2013:fig. 5) reveals that this had a great posterior enlargement of the skull due to the combined extension of the jugal, the squamosals (which still form a squamosal arch but are deeply excavated anteriorly in dorsal view), and, ventrally, by a discrete extension of the ventral process of the pterygoids (based on the holotype). The posterior enlargement of the skull of *Aristonectes quiriquinensis* involves both the pterygoids and the squamosals.

Based on the two pterygoid types ('A' and 'B') proposed by Carpenter (1997:fig. 9), the aristonectine skulls are extended posterior to the occipital condyle as occurs in *Pistosaurus, Liopleurodon*, and *Libonectes* (i.e., type 'A'), differing from the shorter extension observed in *Dolychorhynchops* (type 'B'). Such posterior extension is the type 'A' proposal of Carpenter (1997), but the configuration of the elements along the midline is the modal morphology observed in elasmosaurids, having an anteroposteriorly long basisphenoid between the posterior interpterygoid vacuities, which are also extended in the same direction (O'Keefe, 2001). The large posterior interpterygoid vacuities have a soft and dorsoventrally rounded posterior end that reaches the limit of the atlas-axis anteroventral lip, leaving the internal surface of the interpterygoid vacuities coplanar with the dorsal surface of the axial skeleton.

Inferred Anatomy of the Trigeminal Nerve—*Aristonectes quiriquinensis* possesses a large space for a broad mandibular nerve (6 mm in diameter). In addition, a large trigeminal ganglion is expected based in the internal cast of the trigeminal fossa. Both features can be considered as proxies of for high facial sensitivity; for example, mechanoreception and other sensory input. This condition has been previously found in the extant *Alligator mississippiensis*, indicating a positive correlation between the trigeminal ganglion, the endocast volume, and the skull length (George and Holliday, 2013). On the other hand, there are differences in the degree of ramifications of the mandibular nerve, which in *Alligator mississipiensis* has numerous

neurovascular foramina, contrary to the lizard-like 'linear' pattern here observed in *Aristonectes quiriquinensis*. The ramified pattern was used as osteological correlate to the presence of dome pressure receptors (DPRs) in fossil crocodylians (Soares, 2002), and in the case of the studied material, the single and broad connection between the labial foramina and the mandibular nerve supports the existence of a different sensory device. The labial location of the latter, the large and oval contour of each foramen, and the large number of these foramina observed in the symphyseal portion suggest the associated presence of a single sensory device on each foramen that concentrates a large amount of axons (Kandel et al., 2000). This contrasts with the neurovascular rostral complex recognized in pliosaurids. In particular, in *Pliosaurus kevani*, from the lower Kimmeridgian of England (Benson et al., 2013), the evidence obtained from computed tomography shows the presence of high concentrations of peripheral ramifications in the rostral part of the skull, suggesting the existence of a sensory system likely similar to the crocodile DPRs (Foffa et al., 2014). On the other hand, O'Gorman and Gasparini (2013) studied the unusual dentary grooves present in the polycotylid *Sulcusuchus erraini* from the upper Campanian–lower Maastrichtian of Argentina, suggesting one interpretation of these as special structures of an electrosensitive and/or mechanosensitive nature. The condition in *Aristonectes quiriquinensis* adds a likely third different type of sensorial device among plesiosaurians.

Axial Formula—The preserved neck of SGO.PV.957 allows a more precise estimation of the total number of cervical vertebrae in *Aristonectes quiriquinensis*. Forty-three cervical vertebrae are estimated for this specimen based on the actual count of centra, isolated neural spines, and isolated, incomplete centra recovered. This is a very similar number to those of the aristonectine *Kaiwhekea katiki* from the lower Maastrichtian of New Zealand (Cruickshank and Fordyce, 2002). The juvenile specimen SGO.PV.260 referred to the same species has excellent preservation of the trunk, allowing the count of three pectoral centra and 23 or 24 dorsal vertebrae. Sacral centra are difficult to identify due to the preservation of the referred specimen SGO.PV.260. Based on the isolated sacral ribs (only 'ribs' in Otero et al., 2012:fig. 10d) that can be identified by their dorsoventrally flattened distal portion, the number of sacral centra could be two or three. Finally, SGO.PV.260 preserves most of the tail, except for few anterior caudal centra that seem to be missing. This section is complemented with the specimen SGO.PV.94, allowing an estimate of 35 total centra for the caudal portion (Otero, 2014).

Neck with Neural Spines and Cervical Ribs Recurved Rostrally—Among the vast diversity of fossil reptiles, the presence of cervical neural spines recurved posteriorly is a common feature of terrestrial forms, with a few exceptions having straight neural spines depending on the position of the vertebra (Romer, 1956: fig. 121). Among sauropterygians, an exception are the aristonectines, which have neural arches strongly recurved anteriorly at least in the known specimens preserving that region (Cruickshank and Fordyce, 2002; Otero et al., 2012; Benson and Druckenmiller, 2014; Otero et al., 2014c). Among terrestrial reptiles (and terrestrial vertebrates, in general), the effort involved in the raising of the neck over the body is correlated with the morphology of the dorsal portion of the neural spines. In this sense, neural arches recurved posteriorly provide a better mechanical resistance to such strain. Considering the exclusively aquatic lifestyle of plesiosaurs (O'Keefe and Chiappe, 2011), a functional explanation could be related to a 'reverse' condition where the head is frequently placed deeper with respect to the rest of the body. The neural spines (and cervical ribs) recurved anteriorly certainly could work in analogy to terrestrial vertebrates for keeping the trunk higher than the head, reinforced by an advantage in the buoyancy provided by the aquatic environment, which allows

suspending the body. Such behavior and the postcranial osteological evidence are also consistent with the restricted movement of the atlas-axis, which is unable to move laterally or ventrally with respect to the head (see description).

Hemispherical Head of the Propodials—Prior to our study, the presence of articular hemispherical heads has been described in the femora of other Weddellian forms (Hector, 1874; Welles, 1962; Cruickshank and Fordyce, 2002; Hiller et al., 2005). This condition is clearly present in the humeri of *Aristonectes quiriquinensis* and likely in the femur, based on a complete femur (SGO.PV.135) that precisely matches the distal portion of the holotype (Otero, O'Gorman, and Hiller, 2015). The presence of this feature is known to occur in extant marine vertebrates, particularly in dolphins of the genus *Pontoporia* (Strickler, 1978:fig. 2), which possess a broad ability for propodial movement in the water.

Paleobiological Aspects

Correlation of Osteological Features with Ethology—Emerging cranial features of *Aristonectes quiriquinensis* make plausible the following abilities: engulfing of a large volume of water (with prey) due the large oral space; specialized teeth with very fine crowns, which are not suitable for fish biting. The teeth are recurved rostrally, providing an occlusion inconsistent with prey catching, and maximum gape angle less than 20°, precluding the ingestion of large prey, as well as large gastric stones. On the other hand, postcranial features are consistent with the following abilities: the rostral extension of the anteroventral articular face of the atlas-axis cup and the contact of the atlas-axis ribs with the following first cervical indicate a reduced lateral and ventral movement of the skull with respect to the neck, suggesting poor ability for fast movement and rapid prey catching; cervical ribs and neural spines recurved rostrally suggest the ability to keep the body over the head; hemispherical propodials suggest extremities with a broad range of movement and high maneuverability, as in pontoporiid odontocetes (Strickler, 1978); very large extremities (at least based on the forelimb), with limb/body proportions similar to those of the extant humpback whale (*Megaptera novaeangliae*). These features correlate with slow movements but high maneuverability and suggest a feeding strategy similar to filter feeding, as occurs in *M. novaeangliae* (Fish and Battle, 1995); inferred presence of a horizontal caudal fin with vertical movement based on the caudal features of the axial skeleton. Osteological caudal features are similar to those of extant manatees. A horizontal caudal fin plus large front and hind limbs adds to a high manueverability and slow movements such as those of extant mysticetes.

O'Gorman et al. (2014c) described a large gastrolith set (739 stones) in an aristonectine specimen from Antarctica. Within this clade, this is the only documented case of a large number of gastroliths. On the other hand, the two skeletons of *Aristonectes quiriquinensis* from central Chile preserve a few gastroliths only. The holotype SGO.PV.957 preserves five stones under 70 mm, and SGO.PV.260 (referred specimen) has less than ten stones under 30 mm in diameter. Interestingly, SGO.PV.957 has a disarticulated trunk; however, SGO.PV.260 is a well-articulated skeleton with its entire trunk in anatomical position. This suggests that gastroliths were indeed scarce in *Aristonectes quiriquinensis*; such a feature could be an emergent condition with respect to other aristonectines, at least based on the large number of gastroliths found in the specimen from Antarctica (O'Gorman et al., 2014c). Moreover, the restricted mouth opening in *Aristonectes quiriquinensis* and the tooth grid certainly made the ingestion of large stones difficult.

Feeding Behavior—The evidence presented above suggests the adoption of a combined engulfment and feeding of small (cm-sized) prey from the benthic zone. Previous to this research, engulfment feeding from the benthos was not documented

among reptiles except in *M. seymourensis* (O'Keefe et al., 2017). Benthos feeding in plesiosaurs has been suggested, based on large traces over marine bottom deposits of Callovian age in Switzerland, having been caused by large 'pliosauroids' (Geister, 1998). In addition, the stomach contents of elasmosaurid plesiosaurs from the upper Albian of Australia include one specimen with benthic invertebrates such as bivalves, gastropods, and crinoids, whereas free-swimming taxa are represented by fragments of belemnites and bony fishes; a second specimen includes decapod remains and fish scales (McHenry et al., 2005). Despite the classical understanding of elasmosaurids as specialized in the capture of free-swimming prey, this evidence shows a mixed diet that includes bottom-dwelling organisms. Diverse feeding strategies are indeed documented in Diapsida. Among pterosaurs, the genera *Ctenochasma* and *Pterodaustro* had functional teeth adapted as filaments for filter feeding (Welnhofer, 1991). Among early marine diapsids there are records that originally referred to filter feeding behavior as in the case of *Atopodentatus unicus* Cheng et al. 2014, a marine reptile from the Triassic of China with a drastically modified skull initially interpreted as similar to extant flamingos. However, this was recently reassessed as a marine herbivore with a hammerhead skull (Chun et al., 2016).

Paleoecological Conditions of the Quiriquina Formation—Aristonectines were very large marine reptiles especially abundant in the Quiriquina Formation of central Chile. Conditions supporting such large predatory animals indicate a high availability of prey. The known fossil record from the Quiriquina Formation has shown that bony fishes, the classic prey candidates for elasmosaurids, are scarce (Wilckens, 1904; Wetzel, 1930; Suárez et al., 2003). This could represent a possible taphonomic bias; however, the whole unit is marine and includes different facies representing several environments. The lithologies indicate limestones and sandstones deposited in relatively quiet and shallow waters. On the other hand, tempestites and conglomerates are also present in the unit and indicate high energy tides (Stinnesbeck, 1986). Even with these different conditions, bony fishes appear as a scarce faunal component in all known facies of the unit, contrary to chondrichthyans, which are very abundant in different facies (Suárez et al., 2003). On the other hand, decapods from the Quiriquina Formation are represented by at least two taxa (Stinnesbeck, 1986; Förster and Stinnesbeck, 1987). Trace-bearing levels do occur in most Campanian–Maastrichtian outcrops of the Arauco Basin (where the Quiriquina Formation occurs), ranging ca. 550 km (Tavera, 1980, 1988). This suggests a persistent abundance of decapods throughout the entire Maastrichtian along the whole basin.

Additionally, finds of partial carapaces and chelipeds of *Protocallianasa saetosa* Förster and Stinnesbeck, 1987 joined together in life position, as well as similar remains of *Homolopsis chilensis* Förster and Stinnesbeck, 1987, are quite frequent in the Quiriquina Formation where *Aristonectes quiriquinensis* remains are common. Such carapace remains also show evidence of chemical decomposition (R.A.O., pers. observ., 2013), and these could represent digested remains. Decapod traces (*Thalassinoides* isp. and *Ophiomorpha* isp.) are the most common ichnofossils in the unit, being frequent in several strongly bioturbated strata representing shallow facies (Stinnesbeck, 1986). These observations suggest that shrimp-like decapods were a major available prey source for aristonectines and other organisms in the paleoecosystem represented by the Quiriquina Formation. In the particular case of *Aristonectes quiriquinensis*, the skull and neck features described here are more consistent with this kind of diet as opposed to a typical piscivorous diet. All of these sources of information suggest that *Aristonectes quiriquinensis* adapted to a preferred bottom benthic feeding; however, the presented evidence shows that this taxon could also fed from other small, soft prey in the water column.

Regarding the conditions on the Antarctic Peninsula, the coeval local abundance of aristonectines is comparatively reduced.

However, there is a discrete diversity represented at least by *Aristonectes* sp. (O'Gorman et al., 2013) and (*Morturneria seymourensis* (Chatterjee and Small, 1989). Upper Maastrichtian decapods from Antarctica are known by two genera and represented by a few tens of specimens (Tshudy and Feldmann, 1988), whereas abundant decapod trace levels such as those of the Quiriquina Formation are not observed in the López de Bertodano Formation. Even if this is a taphonomic bias, in addition to these sources of information, the paleomagnetic framework on the Antarctic Peninsula and the South Shetlands indicates a very low apparent polar wandering of the Antarctic Peninsula for the last 100 Ma (Poblete et al., 2011). This evidence is remarkable, because it indicates that light conditions during the late Maastrichtian were very similar to those of today. Near latitude 65°S (Seymour Island), there are nearly 6 months of daylight and few daily hours of night and 6 months of night with few daily hours of light, affecting the productivity of the sea during each season. The histological analysis of the *Aristonectes quiriquinensis* holotype shows synchronization and reinforcement between inherent growth rhythms, food availability, and seasonal cycles, thus indirectly supporting the existence of well-marked seasons during the life of the studied individual (Ossa-Fuentes and Otero, 2014). All of these data suggest that aristonectines could have had migratory routes between Antarctica and South America.

CONCLUSIONS

The skull of *Aristonectes quiriquinensis* represents one of the most derived elasmosaurids known. The posterior expansion of the skull to surround the anterior cervical region is consistent with an increased oral space that allows the engulfment of a large volume of water and prey. This feature could indicate that prey is obtained through an approximate concentration of hidden inside the sediments or that feeding occurs from the benthos on the surface that may end up capturing the sediment together with prey.

The deep symphyseal pit on the mandible is consistent with a strong attachment of the geniohyoid muscle, indirectly suggesting the existence of a loose oral floor. The broad sections of the labial foramina are directly connected to the mandibular nerve cavity, suggesting the presence of sensory devices different from nervous ramified structures such the DPRs in crocodilians (George and Holliday, 2013). In addition, the high number of small teeth oriented rostrally and the reduced angle for mouth opening are not suitable for fish catching but consistent with the catching of small benthic prey. Osteological features of the posterior portion of the skull, the atlas-axis, and the first cervical vertebrae indicate a reduced lateral movement of the skull as well as its ventral bending with respect to the neck. The postcranial features include very large limbs and a dorsoventrally compressed, horizontally expanded tail, similar to a few extant vertebrates with a low stroke frequency (e.g., humpback whale). Environmental and taphonomic conditions of the Quiriquina Formation during the Maastrichtian demonstrate that an abundance of shrimp-like decapods (traces of *Thalassinoides* isp., *Ophiomorpha* isp., and less frequent skeletal remains of *Protocallianasa saetosa* and *Homolopsis chilensis*) contrasts with scarce remains of bony fish in the unit. All of these sources of evidence point to a novel behavior among elasmosaurids, consisting of a mixed engulfing and feeding from the benthic zone. As a similar example, feeding from benthic sediment is documented in the extant grey whale (Ray and Schevill, 1974). These adaptations occurred among marine reptiles at least 30 Ma prior to the appearance of mysticete whales, filling a similar ecomorphotype and likely using migratory routes between Antarctica and southern South America in a way similar to that of several extant mysticetes (such as the humpback whale *Megaptera novaeangliae*) today.

ACKNOWLEDGMENTS

LITERATURE CITED

Andrews, C. W. 1910. A Descriptive Catalogue of the Marine Reptiles of the Oxford Clay, Part I. British Museum (Natural History), London, U.K., 205 pp.

Araújo, R., M. J. Polcyn, J. Lindgren, L. L. Jacobs, A. S. Schulp, I. Mateus, A. Olímpio Gonçalves, and M.-L. Morais. 2015. New aristonectine elasmosaurid plesiosaur specimens from the Early Maastrichtian of Angola and comments on paedomorphism in plesiosaurs. Netherlands Journal of Geosciences. doi: 10.1017/njg.2014.43.

Benson, R. B. J., and P. S. Druckenmiller. 2014. Faunal turnover of marine tetrapods during the Jurassic–Cretaceous transition. Biological Reviews 89:1–23.

Benson, R. B. J., Evans, M., and P. S. Druckenmiller. 2012a. High diversity, low disparity and small body size in plesiosaurs (Reptilia, Sauropterygia) from the Triassic–Jurassic boundary. PLoS ONE 7:e31838.

Benson, R. B. J., Ketchum, H. F., Naish, D., and L. E. Turner. 2012b. A new leptocleidid (Sauropterygia, Plesiosauria) from the Vectis Formation (early Barremian–early Aptian; Early Cretaceous) of the Isle of Wight and the evolution of Leptocleididae, a controversial clade. Journal of Systematic Palaeontology 11:233–250.

Benson, R. B. J., M. Evans, A. S. Smith, J. Sassoon, S. Moore-Faye, H. F. Ketchum, and R. Forrest. 2013. A giant pliosaurid skull from the Late Jurassic of England. PLoS ONE 8(5):e65989. doi:10.1371/journal.pone.0065989.

Biró-Bagóczky, L. 1982. Revisión y redefinición de los 'Estratos de Quiriquina', Campaniano–Maastrichtiano, en su localidad tipo, en la Isla Quiriquina, 36°37′ Lat. Sur, Chile, Sudamérica, con un perfil complementario en Cocholgüe. Congreso Geológico Chileno No. 3 (Concepción), Actas 1, A29–A64.

Blainville, H. M. D. de. 1835. Description de quelques espèces de reptiles de la Californie précédé de l'analyse d'un système général d'herpétologie et d'amphibiologie. Nouvelles Annales du Muséum d'Histoire Naturelle de Paris, Série 3 4:233–296.

Buchholtz, E. A., A. C. Booth, and K. E. Webbink. 2007. Vertebral anatomy in the Florida manatee, *Trichechus manatus latirostris*: a developmental and evolutionary analysis. The Anatomical Record 290:624–637.

Cabrera, A. 1941. Un Plesiosaurio nuevo del Cretáceo del Chubut. Revista del Museo de La Plata 2:113–130.

Carpenter, K. 1997. Comparative cranial anatomy of two North American Cretaceous plesiosaurs; pp. 191–216 in J. M. Callaway and E. Nicholls (eds.), Ancient Marine Reptiles. Academic Press, San Diego, California.

Carpenter, K. 1999. Revision of North American elasmosaurs from the Cretaceous of the Western Interior. Paludicola 2:148–173.

Chatterjee, S., and B. J. Small. 1989. New plesiosaurs from the Upper Cretaceous of Antarctica; pp. 197–215 in J. A. Crame (ed.), Origins and Evolution of the Antarctic Biota. Geological Society of London, Special Publication 47, London, U.K.

Cheng, L., X.-H. Chen, Q.-H. Shang, and X.-C. Wu. 2014. A new marine reptile from the Triassic of China, with a highly specialized feeding adaptation. Naturwissenschaften 101:251–259.

Chun, L., O. Rieppel, C. Long, and N. C. Fraser. 2016. The earliest herbivorous marine reptile and its remarkable jaw apparatus. Science Advances 2:e1501659. doi: 10.1126/sciadv.1501659.

Cope, E. D. 1869. Synopsis of the extinct Batrachia, Reptilia and Aves of North America. Transactions of the American Philosophical Society, New Series 14:1–252.

Cruickshank, A. R., and R. E. Fordyce. 2002. A new marine reptile (Sauropterygia) from New Zealand: further evidence for a Late Cretaceous austral radiation of cryptocleidid plesiosaurs. Palaeontology 45:557–575.

Druckenmiller, P. S., and A. P. Russell. 2008. A phylogeny of Plesiosauria (Sauropterygia) and its bearing on the systematic status of *Leptocleidus* Andrews, 1922. Zootaxa 1863:1–120.

Fish, F. E., and J. M. Battle. 1995. Hydrodynamic design of the humpback whale flipper. Journal of Morphology 225:51–60.

Foffa, D., J. Sassoon, A. R. Cuff, M. N. Mavrogordato, and M. J. Benton. 2014. Complex rostral neurovascular system in a giant pliosaur. Naturwissenschaften 101:453–456.

Förster, R., and W. Stinnesbeck. 1987. Zwei neue Krebse, *Callianasa saetosa* n. sp. und *Homolopsis chilensis* n. sp. (Crustacea, Decapoda) aus der Oberkreide Zentral-Chiles. Mitteilungen der Bayerischen Staatssammlung für Paläontologie und historische Geologie 27:51–65.

Fraas, E. 1910. Plesiosaurier aus dem oberen Lias von Holzmaden. Palaeontographica 57:105–140.

Gasparini, Z., N. Bardet, J. E. Martin, and M. Fernández. 2003. The elasmosaurid plesiosaur *Aristonectes* Cabrera from the latest Cretaceous of South America and Antarctica. Journal of Vertebrate Paleontology 23:104–115.

Geister, J. 1998. Lebensspuren von Meersaurien und ihren Beutetieren im mittleren Jura (Callovien) von Liesburg, Schweiz. Facies 39:105–124.

George, I. D., and C. M. Holliday. 2013. Trigeminal nerve morphology in *Alligator mississippiensis* and its significance for crocodyliform facial sensation and evolution. The Anatomical Record 296:670–680.

Goloboff, P., J. Farris, and K. Nixon. 2003. T.N.T.: Tree Analysis Using New Technology. Program and documentation. Available at www.zmuc.dk/public/phylogeny. Accessed February 14, 2016.

Groβmann, F. 2007. The taxonomic and phylogenetic position of the Plesiosauroidea from the Lower Jurassic Posidonia Shale of southwest Germany. Palaeontology 50:545–564.

Hector, J. 1874. On the fossil reptiles of New Zealand. Transactions of the New Zealand Institute 6:333–358.

Hiller, N., and A. Mannering. 2004. Elasmosaur (Reptilia: Plesiosauria) skull remains from the Upper Cretaceous of North Canterbury. Records of the Canterbury Museum 18:1–7.

Hiller, N., A. Mannering, C. Jones, and A. R. I. Cruickshank. 2005. The nature of *Mauisaurus haasti* Hector, 1874 (Reptilia: Plesiosauria). Journal of Vertebrate Paleontology 25:588–601.

Hopson, J. A. 1979. Paleoneurology; pp. 39–146 in C. Gans (ed.), Biology of the Reptilia, Volume 9, Neurology A. Academic Press, London, U.K.

Kandel, E., J. Schwartz, and T. Jessell. 2000. Principles of Neural Science, 4th edition. McGraw-Hill, New York, New York, 1,414 pp.

Ketchum, H. F., and R. B. J. Benson. 2010. Global interrelationships of Plesiosauria (Reptilia, Sauropterygia) and the pivotal role of taxon sampling in determining the outcome of phylogenetic analyses. Biological Reviews 85:361–392.

Lomax, D. R., and W. R. Wahl. 2013. A new specimen of the elasmosaurid plesiosaur *Zarafasaura oceanis* from the Upper Cretaceous (Maastrichtian) of Morocco. Paludicola 9:97–109.

McHenry, C. R., A. G. Cook, and S. Wroe. 2005. Bottom-feeding plesiosaurs. Science 310:75.

O'Gorman, J. P., and Z. Gasparini. 2013. Revision of *Sulcusuchus erraini* (Sauropterygia, Polycotylidae) from the Upper Cretaceous of Patagonia, Argentina. Alcheringa 37:163–176.

O'Gorman, J. P., Z. Gasparini, and L. Salgado. 2013. Postcranial morphology of *Aristonectes* Cabrera, 1941 (Plesiosauria, Elasmosauridae) from the Upper Cretaceous of Patagonia and Antarctica. Antarctic Science 25:71–82.

O'Gorman, J. P., Z. Gasparini, and L. Salgado. 2014a. Reappraisal of *Tuarangisaurus? cabazai* (Elasmosauridae, Plesiosauria) from the Upper Maastrichtian of northern Patagonia, Argentina. Cretaceous Research 47:39–47.

O'Gorman, J. P., R. A. Otero, and N. Hiller. 2014b. A new record of an aristonectine elasmosaur (Plesiosauria, Elasmosauridae) from the Upper Cretaceous of New Zealand, and the implications for the *Mauisaurus haasti* Hector, 1874 hypodigm. Alcheringa 38:1–8.

O'Gorman, J. P., E. B. Olivero, S. Santillana, M. J. Everhart, and M. Reguero. 2014c. Gastroliths associated with an *Aristonectes* specimen (Plesiosauria, Elasmosauridae), López de Bertodano Formation (upper Maastrichtian) Seymour Island (Is. Marambio), Antarctic Peninsula. Cretaceous Research 50:228–237.

O'Keefe, F. R. 2001. A cladistic analysis and taxonomic revision of the Plesiosauria (Reptilia: Sauropterygia). Acta Zoologica Fennica 213:1–63.

O'Keefe, F. R. 2004. On the cranial anatomy of the polycotylid plesiosaurs, including new material of *Polycotylus latipinnis*, Cope, from Alabama. Journal of Vertebrate Paleontology 24:326–340.

O'Keefe, F. R., and L. M. Chiappe. 2011. Viviparity and K-selected life history in a Mesozoic marine plesiosaur (Reptilia, Sauropterygia). Science 333:870–873.

O'Keefe, F. R., and H. P. Street. 2009. Osteology of the cryptocleidoid plesiosaur *Tatenectes laramiensis*, with comments on the taxonomic status of the Cimoliasauridae. Journal of Vertebrate Paleontology 29:48–57.

O'Keefe, F. R., and W. Wahl. 2003. Preliminary report on the cranial osteology and relationships of a new cryptocleidoid plesiosaur from the Sundance Formation, Wyoming. Paludicola 4:48–68.

O'Keefe, F. R., H. P. Street, B. C. Wilhelm, C. D. Richards, and H. Zhu. 2011. A new skeleton of the cryptoclidid plesiosaur *Tatenectes laramiensis* reveals a novel body shape among plesiosaurs. Journal of Vertebrate Paleontology 31:330–339.

O'Keefe, F. R., R. A. Otero, S. Soto-Acuña, J. P. O'Gorman, S. J. Godfrey, and S. Chatterjee. 2017. Cranial anatomy of *Morturneria seymourensis* from Antarctica, and the evolution of filter feeding in plesiosaurs of the austral Late Cretaceous. Journal of Vertebrate Paleontology. doi: 10.1080/02724634.2017.1347570.

Osborn, H. F. 1903. The reptilian subclasses Diapsida and Synapsida and the early history of the Diaptosauria. Memoirs of the American Museum of Natural History 1:451–507.

Ossa-Fuentes, L., and R. A. Otero. 2014. Microestructura ósea asociada a estadios ontogenéticos de la especie *Aristonectes quiriquinensis* (Plesiosauria, Elasmosauridae), del Maastrichtiano tardío de la Formación Quiriquina, Chile central. IV Simposio – Paleontología en Chile, Valdivia, Chile. Libro de Resúmenes, p. 93.

Otero, R. A. 2014. The axial formula of *Aristonectes quiriquinensis* and its diagnostic value for aristonectines. 74° Meeting of the Society of Vertebrate Paleontology, Berlin, 200 pp.

Otero, R. A. 2016. Taxonomic reassessment of *Hydralmosaurus* as *Styxosaurus*: new insights on the elasmosaurid neck evolution throughout the Cretaceous. PeerJ 4:e1777.

Otero, R. A., and J. P. O'Gorman. 2013. Identification of the first postcranial skeleton of Aristonectes Cabrera (Plesiosauroidea, Elasmosauridae) from the upper Maastrichtian of the south-eastern Pacific, based on a bivariate graphic analysis. Cretaceous Research 41:86–89.

Otero, R. A., J. P. O'Gorman, and N. Hiller. 2015. Reassessment of the upper Maastrichtian material from Chile referred to *Mauisaurus* Hector, 1874 (Plesiosauroidea: Elasmosauridae) and the taxonomical value of the hemispherical propodial head among austral elasmosaurids. New Zealand Journal of Geology and Geophysics 58:252–251.

Otero, R. A., S. Soto-Acuña, and D. Rubilar-Rogers. 2012. A postcranial skeleton of an elasmosaurid plesiosaur from the Maastrichtian of central Chile, with comments on the affinities of Late Cretaceous plesiosauroids from the Weddellian Biogeographic Province. Cretaceous Research 37:89–99.

Otero, R. A., S. Soto-Acuña, A. O. Vargas, and D. Rubilar-Rogers. 2014a. A new postcranial skeleton of an elasmosaurid plesiosaur from the Upper Cretaceous of central Chile and reassessment of the historic species *Cimoliasaurus andium* Deecke. Cretaceous Research 50:318–331.

Otero, R. A., J. P. O'Gorman, N. Hiller, F. R. O'Keefe, and R. E. Fordyce. 2016. *Alexandronectes zealandiensis*, a new aristonectine plesiosaur from the lower Maastrichtian of New Zealand. Journal of Vertebrate Paleontology. doi: 10.1080/02724634.2016.1054494.

Otero, R. A., S. Soto-Acuña, A. O. Vargas, D. Rubilar-Rogers, R. Yury-Yáñez, and C. S. Gutstein. 2014b. Additions to the diversity of elasmosaurid plesiosaurs from the Upper Cretaceous of Antarctica. Gondwana Research 26:772–784.

Otero, R. A., S. Soto-Acuña, F. R. O'Keefe, J. P. O'Gorman, W. Stinnesbeck, M. E. Suárez, D. Rubilar-Rogers, S. Salazar, and L. A. Quinzio. 2014c. *Aristonectes quiriquinensis* sp. nov., a new highly derived elasmosaurid from the upper Maastrichtian of central Chile. Journal of Vertebrate Paleontology 34:100–125.

Owen, R. 1860. On the orders of fossil and recent Reptilia and their distribution in time. Report of the British Association for the Advancement of Science 29:153–166.

Poblete, F., C. Arriagada, P. Roperch, N. Astudillo, F. Hervé, S. Kraus, and J. P. Le Roux. 2011. Paleomagnetism and tectonics of the South Shetland Islands and the northern Antarctic Peninsula. Earth and Planetary Science Letters 302:299–313.

Ray, G. C., and W. E. Schevill. 1974. Feeding of a captive gray whale, *Eschrichtius robustus*. Marine Fisheries Review (NOAA) 36:31–38.

Romer, A. S. 1956. Osteology of the Reptiles. Krieger Publishing Company, Malabar, Florida, 792 pp.

Sachs, S., J. Hornung, and B. Kear. 2016. Reappraisal of Europe's most complete Early Cretaceous plesiosaurian: *Brancasaurus brancai* Wegner, 1914 from the "Wealden facies" of Germany. PeerJ 4: e2813.

Salazar, C., W. Stinnesbeck, and L. A. Quinzio-Sinn. 2010. Ammonites from the Maastrichtian (Upper Cretaceous) Quiriquina Formation in central Chile. Neues Jahrbuch für Geologie und Paläontologie. Abhandlungen 257:81–236.

Sato, T. 2002. Description of plesiosaurs (Reptilia: Sauropterygia) from the Bearpaw Formation (Campanian–Maastrichtian) and a phylogenetic analysis of the Elasmosauridae. Unpublished Ph.D. dissertation, University of Calgary, Calgary, Alberta, Canada, 408 pp.

Smith, A. S. 2013. Morphology of the caudal vertebrae in *Rhomaleosaurus zetlandicus* and a review of the evidence for a tail fin in Plesiosauria. Paludicola 9:144–158.

Smith, A. S., and G. J. Dyke. 2008. The skull of the giant predatory pliosaur *Rhomaleosaurus cramptoni*: implications for plesiosaur phylogenetics. Naturwissenschaften 95:975–980.

Smith, A. S., and P. Vincent. 2010. A new genus of pliosaur (Reptilia: Sauropterygia) from the Lower Jurassic of Holzmaden, Germany. Palaeontology 53:1049–1063.

Soares, D. 2002. An ancient sensory organ in crocodilians. Nature 417:241–242.

Stinnesbeck, W. 1986. Zu den faunistischen und palökologischen Verhältnissen in der Quiriquina Formation (Maastrichtium) Zentral-Chiles. Palaeontographica, Abteilung A 194:99–237.

Stinnesbeck, W. 1996. Ammonite extinctions and environmental changes across the Cretaceous–Tertiary boundary in central Chile; pp. 289–302 in N. MacLeod and G. Keller (eds.), The Cretaceous–Tertiary Boundary Mass Extinction: Biotic and Environmental Events. Norton Press, New York, New York.

Stinnesbeck, W., C. Ifrim, and C. Salazar. 2012. The last Cretaceous ammonites in Latin America. Acta Paleontologica Polonica 57:717–728.

Storrs, G. 1997. Morphological and taxonomical clarification of the genus *Plesiosaurus*; pp. 145–190 in J. M. Callaway and E. Nicholls (eds.), Ancient Marine Reptiles. Academic Press, San Diego, California.

Strickler, T. L. 1978. Myology of the shoulder of *Pontoporia blainvillei*, including a review of the literature on shoulder morphology in the Cetacea. American Journal of Anatomy 152:419–432.

Suárez, M. E., L. A. Quinzio, O. Fritis, and R. Bonilla. 2003. Aportes al conocimiento de los vertebrados marinos de la Formación Quiriquina. Congreso Geológico Chileno No. 10, Concepción. Resúmenes, 7 pp.

Tavera, J. 1980. Cretáceo y Terciario de la Localidad de Algarrobo. Imprentas Gráficas, Santiago, Chile, 45 pp.

Tavera, J. 1988. Formación Quiriquina. Localidades tipo para la Formación. Estratotipos y Fauna (Latitudes 33°21′–37°50′). Monography. Departamento de Geología, Universidad de Chile, Santiago, Chile, 244 pp.

Ten Donkelaar, H. J. 1998. Reptiles; pp. 1315–1524 in R. Nieuwenhuys, H. J. Ten Donkelaar, and C. Nicholson (eds.), The Central Nervous System of Vertebrates, Volume 2. Springer-Verlag, Berlin-Heidelberg, Germany.

Tshudy, D. M., and R. M. Feldmann. 1988. Macrurous decapod crustaceans, and their epibionts, from the López de Bertodano Formation (Late Cretaceous), Seymour Island, Antarctica; pp. 291–301 in R. M. Feldmann and M. O. Woodburne (eds.), Geology and Paleontology of Seymour Island, Antarctica. Geological Society of America, Memoir 169.

Vincent, P., N. Bardet, X. Pereda-Suberbiola, B. Bouya, M. Amaghzaz, and S. Meslouh. 2011. *Zarafasaura oceanis*, a new elasmosaurid (Reptilia: Sauropterygia) from the Maastrichtian Phosphates of Morocco and the palaeobiogeography of latest Cretaceous plesiosaurs. Gondwana Research 19:1062–1073.

Welles, S. P. 1943. Elasmosaurid plesiosaurs with description of new material from California and Colorado. Memoirs of the University of California 13:125–254.

Welles, S. P. 1952. A review of the North American Cretaceous elasmosaurs. University of California Publications in Geological Sciences 29:47–144.

Welles, S. P. 1962. A new species of elasmosaur from the Aptian of Colombia and a review of the Cretaceous plesiosaurs. University of California Publications in Geological Sciences 44:1–96.

Welnhofer, P. 1991. The Illustrated Encyclopedia of Pterosaurs. Barnes and Noble Books, New York, New York, 124 pp.

Wetzel, W. 1930. Die Quiriquina-Schichten als Sediment und paläontologisches archiv. Palaeontographica 73:49–101.

Wiffen, J., and W. Moisley. 1986. Late Cretaceous reptiles (families Elasmosauridae, Pliosauridae) from the Mangahouanga Stream, North Island, New Zealand. New Zealand Journal of Geology and Geophysics 29:205–252.

Wilckens, O. 1904. Revision der fauna der Quiriquina-Schichten. Neues Jahrbuch für Mineralogie, Geologie und Paläontologie, Beilage-Band 18:181–284.

Wilhelm, B. C., and F. R. O'Keefe. 2010. A new partial skeleton of a cryptocleidoid plesiosaur from the Upper Jurassic Sundance Formation of Wyoming. Journal of Vertebrate Paleontology 30:1736–1742.

Zinsmeister, W. 1979. Biogeographic significance of the Upper Mesozoic and early Tertiary molluscan faunas of Seymour Island (Antarctic Peninsula) to the final break-up of Gondwanaland; pp. 349–355 in J. Gray and A. J. Boucot (eds.), Historical Biogeography, Plate Tectonics and the Changing Environment. Oregon State University Press, Eugene, Oregon.